AD_____

Award Number: DAMD17-99-1-9120

TITLE: Comparative Structural Analysis of Erα and Erβ Bound to Selective Estrogen Agonists and Antagonists

PRINCIPAL INVESTIGATOR: Geoffrey L. Greene, Ph.D.

CONTRACTING ORGANIZATION: The University of Chicago
Chicago, Illinois 60637

REPORT DATE: July 2002

TYPE OF REPORT: Final

PREPARED FOR: U.S. Army Medical Research and Materiel Command
Fort Detrick, Maryland 21702-5012

DISTRIBUTION STATEMENT: Approved for Public Release;
Distribution Unlimited

REPORT DOCUMENTATION PAGE

Form Approved
OMB No. 074-0188

1. AGENCY USE ONLY (Leave blank)	2. REPORT DATE	3. REPORT TYPE AND DATES COVERED
	July 2002	Final (14 Jun 99 - 13 Jun 02)

4. TITLE AND SUBTITLE
Comparative Structural Analysis of Erα and Erβ Bound to Selective Estrogen Agonists and Antagonists

5. FUNDING NUMBERS
DAMD17-99-1-9120

6. AUTHOR(S)
Geoffrey L. Greene, Ph.D.

7. PERFORMING ORGANIZATION NAME(S) AND ADDRESS(ES)
The University of Chicago
Chicago, Illinois 60637

E-Mail: ggreene@uchicago.edu

8. PERFORMING ORGANIZATION REPORT NUMBER

9. SPONSORING / MONITORING AGENCY NAME(S) AND ADDRESS(ES)
U.S. Army Medical Research and Materiel Command
Fort Detrick, Maryland 21702-5012

10. SPONSORING / MONITORING AGENCY REPORT NUMBER

11. SUPPLEMENTARY NOTES
report contains color

12a. DISTRIBUTION / AVAILABILITY STATEMENT
Approved for Public Release; Distribution Unlimited

12b. DISTRIBUTION CODE

13. Abstract ***(Maximum 200 Words)*** *(abstract should contain no proprietary or confidential information)*

The goal of this investigation is to determine the three-dimensional structures of the two known human estrogen receptors (ERα and ERβ) complexed with receptor-selective estrogens and antiestrogens (SERMs). The crystallographic structures of ERα and ERβ ligand binding domains complexed with *cis*-R,R-diethyl-tetrahydrochrysene-2,8-diol (R,R-THC) have been solved and refined, suggesting mechanisms by which this compound can act as an ERα agonist and as an ERβ antagonist. Agonists and antagonists bind at the same site within the core of the ER LBD to induce distinct conformations in the transactivation domain (AF-2), especially in the positioning of helix 12. Previously determined structures of ERα with 4-hydroxytamoxifen (OHT) and diethylstilbestrol (DES) revealed and defined a multipurpose docking site on ERα and ERβ that can accommodate either helix 12, in the presence of OHT, or one of several co-regulators in the presence of DES. R,R-THC stabilizes a conformation of the ERα LBD that favors coactivator association and a conformation of the ERβ LBD that prevents coactivator association. A comparison of the two structures, combined with functional data, reveals that THC does not act on ERβ through the same mechanisms used by other known ER antagonists. Instead, THC antagonizes ERβ through a novel mechanism we term "passive antagonism". Paradoxically, the R,R-THC-ERβ structure is very similar to the structure induced by genistein, which acts as a partial estrogen through both ER subtypes. Ongoing mutagenesis studies have helped define some of the molecular and structural differences that are responsible for these unanticipated results. The passive antagonism mechanism, combined with mutagenesis data, suggests a novel approach to the design of ligands that selectively antagonize the two ER subtypes. Such ligands may have therapeutic properties that can be exploited to prevent or treat breast cancer.

14. SUBJECT TERMS	15. NUMBER OF PAGES
estrogen receptors alpha and beta Erα and Erβ, receptor structure, x-ray crystallography, selective estrogen receptor modulators (SERMs), agonism versus antagonism, passive antagonism, breast cancer	31
	16. PRICE CODE

17. SECURITY CLASSIFICATION OF REPORT	18. SECURITY CLASSIFICATION OF THIS PAGE	19. SECURITY CLASSIFICATION OF ABSTRACT	20. LIMITATION OF ABSTRACT
Unclassified	Unclassified	Unclassified	Unlimited

NSN 7540-01-280-5500

Standard Form 298 (Rev. 2-89)
Prescribed by ANSI Std. Z39-18
298-102

Table of Contents

INTRODUCTION

The goal of this investigation was to determine the three-dimensional structures of the two known human estrogen receptors (ERα and ERβ) complexed with receptor-selective estrogens and antiestrogens (SERMs). An important, unresolved issue is the molecular mechanism(s) by which SERMs can act selectively as full agonists, partial agonists, or complete antagonists in the control of cell proliferation and cell fate in different tissues. The physiological effects of both endogenous and synthetic SERMs are mediated by the estrogen receptors (ERs), ERα and ERβ, members of the nuclear receptor (NR) super-family of ligand-regulated transcription factors. The two ER subtypes have overlapping but distinct tissue distribution patterns *in vivo* and distinct activation profiles at both classical and complex promoter elements. Thus, it is unclear how ERα and ERβ individually contribute to the effects of known estrogens. Ligands that act differentially on ERα and ERβ would be potentially valuable both as tools to dissect the biological roles of the two ERs and as novel therapeutics with pharmacological properties distinct from existing drugs. As part of a search for ER subtype-selective ligands, the synthetic compound, R,R-5,11-*cis*-diethyl-5,6,11,12-tetrahydrochrysene-2,8-diol (R,R-THC), was identified as a selective estrogen agonist when bound to ERα and as an antagonist when bound to ERβ. To better understand this selective behavior, a major goal of this investigation was to determine the crystallographic structures of human ERα and ERβ ligand binding domains (LBDs) complexed with R,R-THC. These structures have now been solved and refined, suggesting mechanisms by which this compound can act as an ERα agonist and as an ERβ antagonist.

Previously determined structures of ERα with 4-hydroxytamoxifen (OHT) and diethylstilbestrol (DES) (1) revealed and defined a multipurpose docking site on ERα and ERβ that can accommodate either helix 12, in the presence of OHT, or one of several co-regulators in the presence of DES. Thus, agonists and antagonists bind at the same site within the core of the ER LBD to induce distinct conformations in the transactivation domain (AF-2), especially in the positioning of helix 12. Interestingly, R,R-THC stabilizes a conformation of the ERα LBD that favors coactivator association and a conformation of the ERβ LBD that prevents coactivator association. A comparison of the two structures, combined with functional data, reveals that R,R-THC does not act on ERβ through the same mechanisms used by other known ER antagonists. Instead, R,R-THC antagonizes ERβ through a novel mechanism we term "passive antagonism". Paradoxically, the R,R-THC-ERβ structure is very similar to the structure induced by genistein (2), which acts as a partial estrogen through both ER subtypes. Ongoing mutagenesis studies have helped define some of the molecular and structural differences that are responsible for these unanticipated results. In addition, the passive antagonism mechanism suggests a novel approach to the design of ligands that selectively antagonize the two ER subtypes. Such ligands may have novel therapeutic properties that can be exploited to prevent or treat breast cancer.

This investigation resulted in a major publication (3) (See Appendix) that describes our success in achieving the goals stated in the original proposal. During the third and final year we continued to use site directed mutagenesis to define and characterize residues in the ERα/β LBDs that are responsible for ER subtype-selective ligand recognition. It became clear that ligand discrimination by the two ER subtypes is more complicated than first imagined. As summarized below, our data illustrate that secondary structure interactions and flexibility are key determinants of ligand specificity for the two ER subtypes, revealing novel aspects of nuclear

receptor function. Equally important, residues outside the ligand-binding pocket appear to be critical for ligand discrimination between two closely related nuclear receptors.

BODY

The Statement of Work for this grant listed four major tasks. These tasks are listed below with details of the progress made toward achieving each goal during the past three years.

Task 1 (First year): To produce and purify bacterially expressed ERα-LBD-BJK-1 (R,R-THC) complexes for biochemical analysis and crystallization.

As described in detail in the attached reprint (3) (see Appendix) and in last year's Annual Report, this task has been accomplished. BJK-1 (named after Benita and John Katzenellenbogen) was renamed R,R-THC once we knew its chemical identity.

Task 2 (Second year): Purification, crystallization, and x-ray analysis of ERα/β-LBD-BJK-1 and ERα/β-LBD-ICI complexes.

The major goal, which was to solve the **R,R-THC-ERα/β LBD** structures, has been achieved, as described in the attached reprint (3) (see Appendix). Both structures are discussed in detail below. We did not pursue either the ERα-or ERβ-ICI 182,780 complexes because the R,R-THC studies consumed all available personnel time for this grant. Also, the Hubbard lab solved the structure of rat ERβ LBD complexed with ICI 164,384 in 2001 (4). It may still be of some value to know if the ERα-ICI conformation is different from the published ERβ-ICI conformation. Noteworthy in the ICI-ERβ structure was the absence of any association of the transactivation helix (H12) with the LBD, which contrasts with all other known antagonist-ER structures, in which H12 is associated with the hydrophobic cleft formed by helices 3, 4 and 5 (**Figure 1** and **Appendix, Figure 1b**). In the ICI-ERβ complex, the terminal portion of the ICI bulky side chain substituent emerges from the ligand-binding pocket and binds to part of the coactivator recruitment site (AF2) (**Figure 1c**), thereby preventing H12 from adopting either its

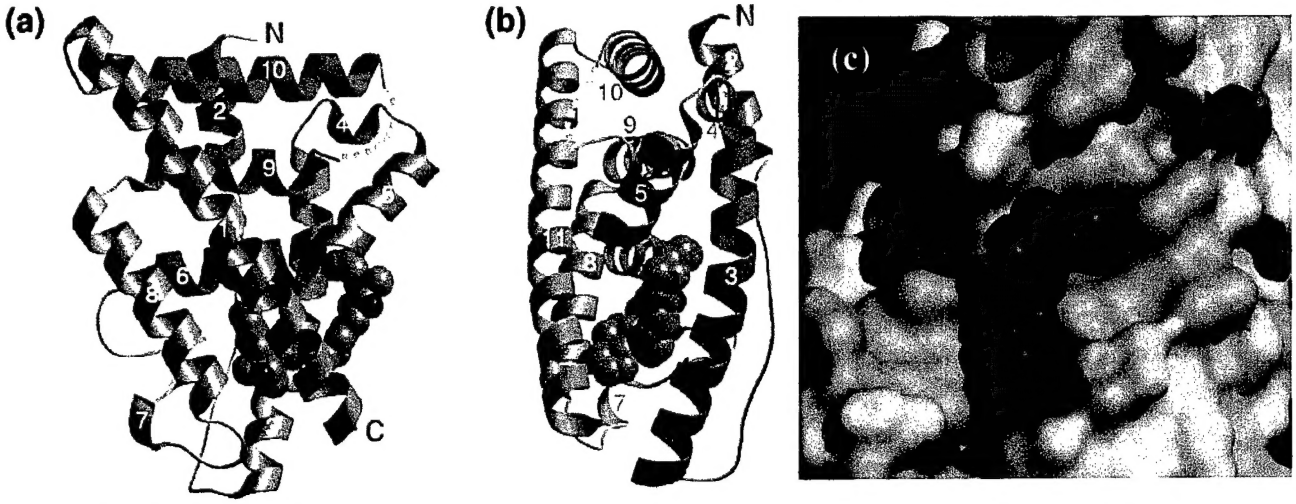

Figure 1. **(a)(b)** Orthogonal views of ERβ-LBD bound to the pure antagonist ICI 164,384. **(c)** Interaction of ICI side chain with coactivator groove. Reproduced from Pike et al. (4).

characteristic agonist or antagonist orientation. This complete destabilization of H12 may contribute to the more potent antiestrogenic activity of both closely related ICI compounds when compared to SERMs like tamoxifen and raloxifene. Another potentially significant difference is the effect of the ICI 164,384 on the ERβ dimerization interface. For all other known ERα/β LBD structures, the ligand has little effect on the nature or extent of the dimer interface. However, ICI appears to generate a more open and perhaps less stable dimer, consistent with reports that ERα-ICI dimers are less stable than other ligand-ER complexes (5). It is also possible that a crystallization artifact is responsible for the observed ICI-induced conformation, or that the ERβ dimer interface is more sensitive than ERα to ligand effects (4). For ERβ-R,R-THC, the dimer interface is very similar to the ERβ-Ral and ERβ-Gen structures (2, 4).

R,R-THC ERα/β structures. Refinement of the R,R-THC-ERα/β LBD structures continued into the early part of year 3, providing additional insights about key structural differences between the two ER subtypes. The overall structures of R,R-THC-ERα LBD and R,R-THC-ERβ LBD are shown in **Figure 2** and in the **Appendix, Figure 1b**. The helices are arranged as in **Figure 1**, except that H12 (shown in red) is structured and either resting across the LBD pocket (**Fig. 2a, ERα**) or in the hydrophobic cleft formed by helices 3-5 (**Figure 2b, ERβ**). Although we were able to obtain preliminary crystallographic solutions for both the R,R-THC-

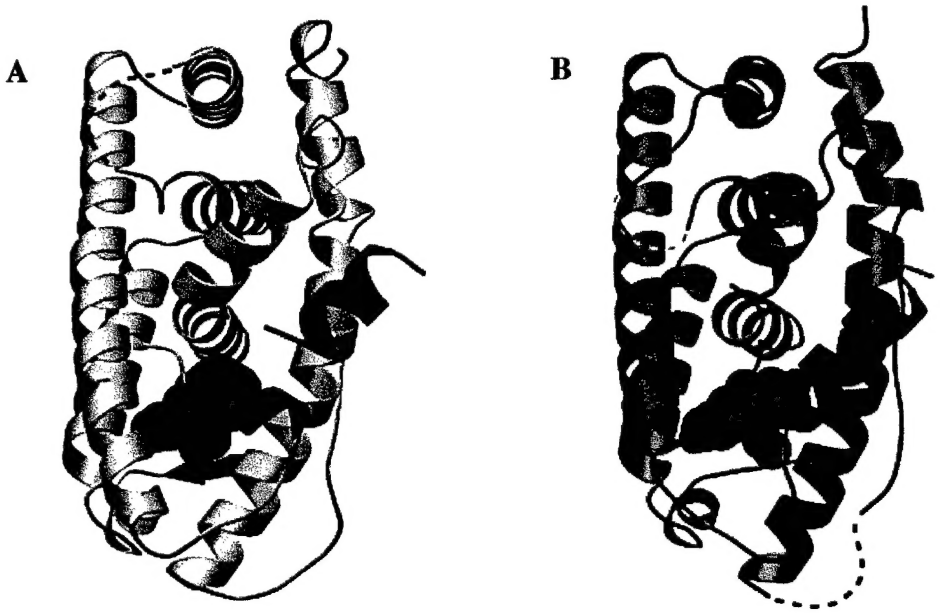

Figure 2. Overall structures of the R,R-THC-ER LBD complexes. **A.** R,R-THC-ERα LBD + GRIP1 NR box II peptide. **B.** R,R-THC-ERβ LBD (**Appendix, Figure 1b**)

ERα and R,R-THC-ERβ LBD structures almost two years ago, ongoing data refinement during the past year revealed a more complex ligand interaction with the ERβ pocket than proposed initially. As shown in **Figure 3**, our original assumption that fewer contacts between R,R-THC and the amino acid residues that line the pocket of ERβ were responsible for the inability of this complex to assume an agonist conformation was incorrect. Instead, an equal number of contacts occur between R,R-THC and amino acids that comprise the ligand-binding pocket, as compared

to the R,R-THC-ERα LBD complex (**Appendix, Figure 3b**). The ERα complex structure has now been refined to a crystallographic R factor of 20.3% (R_{free} = 24.2%) using data to 1.95 Å resolution and the ERβ complex structure has been refined to a crystallographic R factor of 25.9% (R_{free} = 29.9%) using data to 2.95 Å resolution (**Appendix, Table 1**). It proved especially difficult to obtain an R_{free} value of 29.9% for ERβ, which is why we did not initially see the additional contacts that were present between R,R-THC and the ERβ LBD pocket. For example, we did not initially see the additional hydrogen bond that occurs between the A ring phenolic OH of R,R-THC and Arg 346, similar to the interaction with Arg 394 in the R,R-THC-ERα structure (**Figure 3B; Appendix, Figure 3b**). Similarly, additional R,R-THC contacts with the ERβ LBD pocket could only be appreciated upon further refinement of the structural data. We now feel that 16 amino acids, rather than the 11 first observed (**Figure 3B; Appendix, Figure 3b**), participate in the stabilization of R,R-THC in ERβ, which equals the 16 amino acids that are

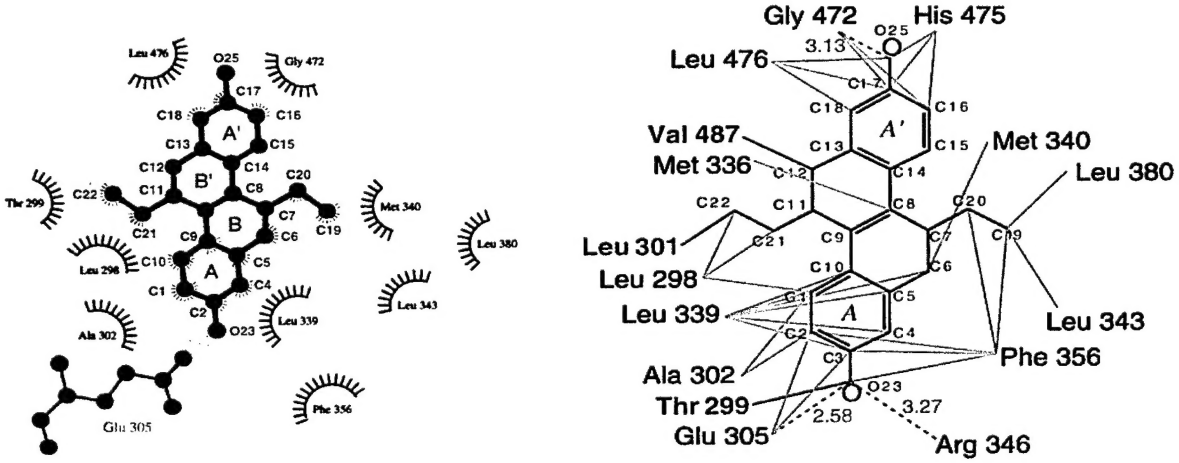

Figure 3. R,R-THC Interactions with ERβ LBD Pocket. **A.** Original model. **B.** Current model based on most refined structure (see **Appendix, Figure 3b**).

involved in the R,R-THC-ERα LBD complex, although not all residues are the same (**Appendix, Figure 3b, 3c**). Also, a water molecule participates in the hydrogen bonds that stabilize the 'A ring' of R,R-THC in the ERα LBD, but not in the ERβ LBD (**Appendix, Figure 3b, 3c**). The R,R-THC-ERα LBD pocket residue interactions are very similar to those of the full agonists estradiol and DES and nucleate all of the polar and nonpolar contacts that are required to favor the agonist-bound conformation of ERα in which helix 12 rests across the pocket (**Figure 2A; Appendix, Figure 1b**).

Thus, although our hypothesis of "passive antagonism" has not changed, our view of the underlying mechanism(s) has evolved. As described previously, the ERβ LBD shares the same overall fold as the ERα LBD (**Figure 2; Appendix, Figure 1b**) (2). And like the ERα LBD, the ERβ LBD recognizes R,R-THC with a ligand-binding pocket located within its lower sub domain. However, the binding of R,R-THC to the ERβ LBD does not stabilize the agonist-bound conformation of helix 12 (**Figure 2; Appendix, Figure 1b**). Also, helix 12 is not bound to the portion of the coactivator recognition groove formed by helices 3, 4, and 5 as it is in the

OHT-ERα LBD (1), RAL-ERα LBD (6), and RAL-ERβ LBD (2) complexes (**Figure 2; Appendix, Figure 2a**), nor is it disordered as it is in the ICI-ERβ LBD complex (**Figure 1**) (4). Instead, helix 12 in the R,R-THC-ERβ LBD complex interacts with the rest of the LBD in a manner most like that observed in the GEN-ERβ LBD complex (**Figure 4; Appendix, Figure 2a**) (2). Helix 12 is positioned similarly, and of comparable length (residues 487 to 498 in the R,R-THC complex and residues 487 to 497 in the GEN complex) in the two structures (**Figure 4; Appendix, Figure 2a**).

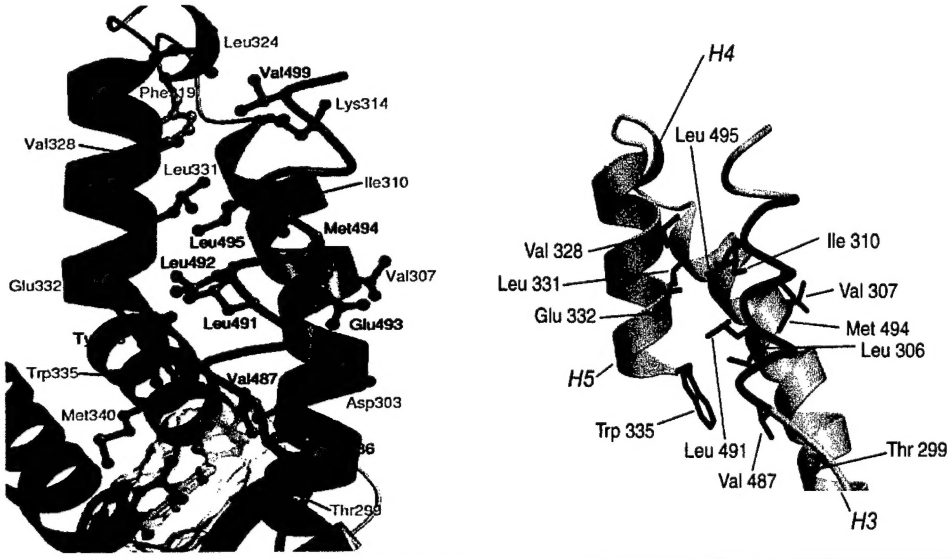

Figure 4. Positioning of H12 in GEN-ERβ LBD (left) and R,R-THC- ERβ LBD (right). GEN-ERβ LBD figure is reproduced from Pike et al. (2).

Based on previous correlations between the positioning of H12 and the ability of ERα and other NRs to form coactivator complexes, the conformation of the ERβ LBD observed in both the R,R-THC and GEN complexes should be incapable of interacting with coactivators and, hence, should be transcriptionally silent for two reasons. First, key residues from helix 12 (Leu 490, Glu 493, and Met 494) that are predicted to form part of the coactivator recognition surface are inappropriately positioned. In addition, helix 12 itself is bound such that it partially occludes the static region of the coactivator-binding surface formed by residues from helices 3, 4, and 5. Yet, GEN and R,R-THC clearly exhibit different activities on ERβ in mammalian cells; GEN acts as a partial agonist (7) and R,R-THC acts as a pure antagonist (8, 9). How can the similarity of the two structures be reconciled with the different activities of these compounds in transcriptional assays? The simplest model that explains these and other data is based on two suppositions (**Figure 5**). First, helix 12 in the unliganded ERβ LBD is in equilibrium between the R,R-THC/GEN-bound conformation, which precludes coactivator association, and the agonist-bound conformation seen in the E2- and DES-ERα LBD structures, which favors coactivator association (with the "inactive" R,R-THC/GEN-bound conformation being heavily favored). Second, rather than stabilizing a single static conformation of helix 12, ligands serve to shift the balance of this equilibrium. It is also highly likely that the coactivator receptor-interaction domain (e.g. GRIP NR box II domain) plays an active role in shifting this equilibrium.

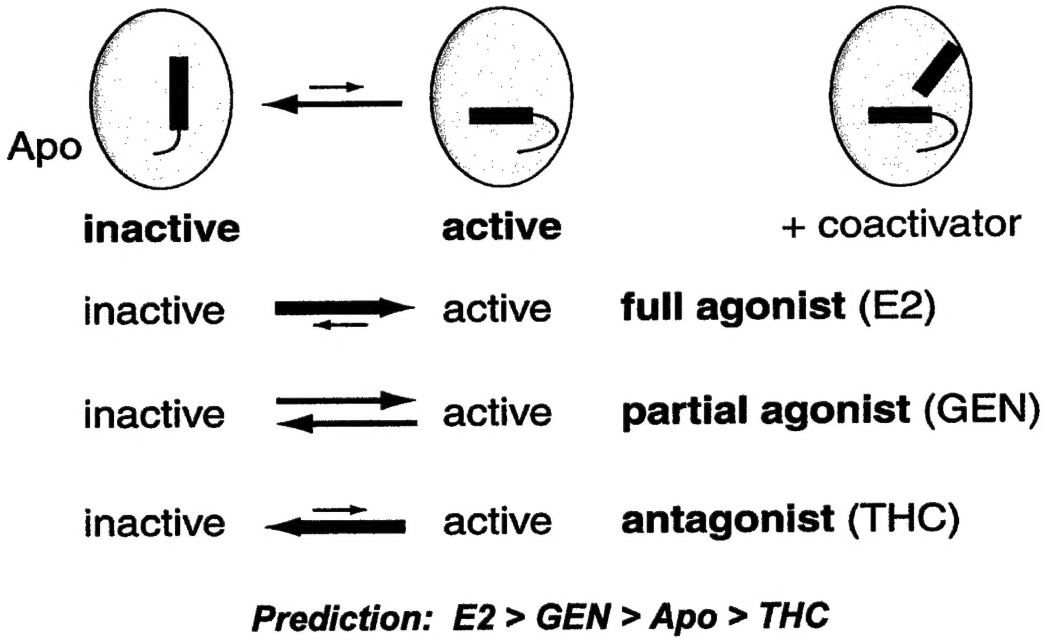

Figure 5. Equilibrium model of Helix 12 positioning.

R,R-THC could antagonize receptor activity by shifting equilibrium in favor of the inactive R,R-THC/GEN-bound conformation (**Figure 5**). If R,R-THC binding forces the receptor to favor this conformation even more than it does in the absence of ligand, the R,R-THC-receptor complex would be expected to have an even lower affinity for coactivator than the unliganded receptor. This would be consistent with the absence of transcriptional activity of the R,R-THC-ERβ complex and the conformation of helix 12 observed in the crystal.

Because the conformational equilibrium of helix 12 would be difficult to observe directly, we chose to test the hypothesis that the binding of different ligands should modulate the affinity of the ERβ LBD for coactivator such that E2-LBD ~ DES-LBD > GEN-LBD > apo-LBD > R,R-THC-LBD. The affinities of various ligand-ERβ LBD complexes for an LXXLL motif-containing peptide were therefore directly measured using a fluorescence polarization-based binding assay (**Appendix, Figure 2b**) (3, 10). The full agonist complexes bind the peptide approximately 1.5-fold more tightly than the GEN complex (K_d[E2] = 71 nM, K_d[GEN] = 104 nM). In addition, the GEN complex binds the peptide more tightly than the unliganded receptor (K_d[apo] = 215 nM), whereas the R,R-THC complex (K_d[R,R-THC] = 3.3 μM) binds the peptide significantly weaker than the unliganded receptor. Thus, these data are entirely consistent with the described helix 12 conformational equilibrium model. Furthermore, recent mutational and crystallographic data suggest that the positioning of helix 12 in ERα (11) and other NRs (12) is also dictated by a ligand-sensitive conformational equilibrium.

To better define and understand "passive antagonism", or antagonism without side chains, one has to consider the differences between classical estrogen antagonists, which contain bulky side

chains, and molecules like R,R-THC. Although agonists and antagonists bind at the same site within the core of the LBD, each induces distinct conformations in the transactivation domain (AF-2) of the LBD, especially in the positioning of helix 12, providing structural evidence for multiple mechanisms of selective antagonism in the nuclear receptor family. Interestingly, the OHT/RAL and DES/E2 structures collectively reveal and define a multipurpose docking site on ERα that can accommodate either helix 12 or one of several coregulators. In addition, a comparison of the two types of structures reveals that there are at least two distinct mechanisms by which structural features of OHT promote an inhibitory conformation of helix 12 (1, 6). Helix 12 positioning is determined both by steric considerations, such as the presence of an extended side chain in the ligand, and by local structural distortions in and around the ligand binding pocket. Thus, one would predict that effective estrogen antagonists do not necessarily require bulky or extended side chains.

The positioning of the side chains of OHT, RAL, and ICI directly or "actively" preclude the agonist-bound conformation of helix 12 by steric hindrance. Hence, we define their common mechanism of action as "active antagonism". Clearly, R,R-THC does not have a bulky side chain (**Appendix, Figure 1a**), and in its complex with ERβ, helix 12 is not sterically precluded from adopting the agonist-bound conformation as it is in the other antagonist complexes (**Figure 2; Appendix, Figures 1b and 2a**). Instead, R,R-THC antagonizes ERβ by stabilizing key ligand binding pocket residues in nonproductive conformations, and disfavoring the equilibrium to the agonist-bound conformation of helix 12 (**Figure 5**). Thus, we term the mechanism of antagonism of R,R-THC as "passive antagonism". Passive antagonism may not be unique to R,R-THC and ERβ. There are many examples of NR ligands, which act as antagonists even though they are smaller than the endogenous agonists of these NRs. The synthetic androgen receptor antagonist, flutamide, is comparable in size to testosterone, and does not possess an obvious moiety that would act as an antagonist side chain (13).

Many NRs have multiple subtypes that possess distinct expression patterns and that regulate distinct target genes. Antagonists generated through the addition of bulky side chains to agonist scaffolds are limited to being antagonistic on one or more subtypes of a particular NR. The passive antagonism mechanism, as revealed in our studies through direct comparison of the two R,R-THC-ER LBD complexes, suggests a new approach to achieving NR antagonism. Compounds could be designed to selectively stabilize the inactive conformations of certain NR subtypes and the active conformations of others. Such ligands may exert novel biological and therapeutic effects.

A manuscript describing the above data was recently published in *Nature Structural Biology* (3). Clearly, significant progress was made during the past three years in our efforts to understand the unique ER subtype-selective behavior of R,R-THC and the R,R-THC-induced conformation of ERβ that contributes to "passive antagonism". More on this subject is included in the summary of Tasks 3 & 4 below.

Tasks 3 & 4 (Third year): To compare and correlate structural differences among hERα/β-LBD complexes with the biological activity of hERα/β.

We have made significant progress in trying to understand the contributions of residues that line the ligand-binding pocket to ligand discrimination between ERα and ERβ. Progress has also been made in our effort to crystallize ERα bound to the unique SERM GW5638. However, the main effort related to this grant during the third year was to better understand what distinguishes ERα from ERβ in their ability to differentially recognize diverse ligands with unique behavior. To achieve this goal, we generated a series of specific mutant ERs and tested their ability to interact with known coactivators and/or corepressors and to act as selective transcription modulators in co-transfection assays. Surprisingly, we discovered that residues outside the ligand-binding pocket play important roles in ligand recognition and discrimination between the two ER subtypes.

As described above, R,R-THC does not behave as an ERβ agonist. Instead, it forms alternative hydrogen bonds and additional packing (van der Waals) contacts not observed in the ERα complex (**Appendix, Figure 3b, 3c**). Hence, R,R-THC is able to bind to the ERβ LBD without nucleating many of the equivalent cooperative interactions observed in the ERα complex. For example, in the ERα complex the side chain of Met 528 packs against the side chains of His 524 and Met 343, stabilizing the helical conformation of the flanking residues. Because R,R-THC binding favors alternative conformations of His 475 and Met 295 (equivalent to His 524 and Met 343, respectively), the side chain of Met 479 (equivalent to Met 528) is completely disordered in the ERβ complex. In fact, by stabilizing conformations of binding pocket residues that prevent their interaction, R,R-THC binding should actually disfavor the equilibrium to the agonist-bound conformation of helix 12 (**Figure 5; Appendix, Figure 2b**).

A key unanswered question relates to the molecular/structural differences between the two ER subtypes that allow R,R-THC to stabilize these distinct arrangements of ligand binding pocket residues. There are only two binding pocket residues which are not identical in the two

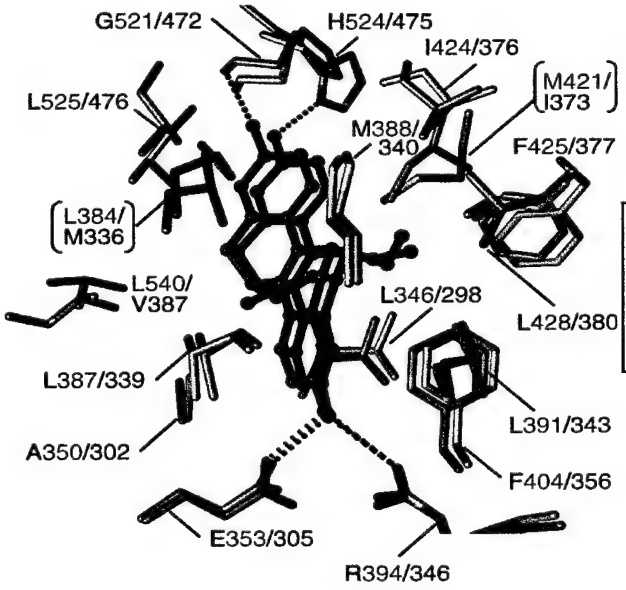

Figure 6. Superimposed binding pockets of ERα and ERβ bound to R,R-THC. Brackets identify residues that are different between the two ER subtypes.

subtypes: Leu 384 (from helix 5/6) and Met 421 (from helix 8) in ERα, which are equivalent to Met 336 and Ile 373, respectively, in ERβ (**Figure 6; Appendix, Figure 3c**) (14, 15). These two residue pairs are similarly positioned on opposite faces of R,R-THC in their respective

complexes. In the ERα complex, Leu 384 and Met 421 form several nonpolar contacts with R,R-THC (**Appendix, Figure 3b**). By contrast, only Met 336 interacts with R,R-THC in the ERβ complex.

The two ligand binding pocket residues that differ between the two subtypes may partially explain the failure of R,R-THC to act as an ERβ agonist. Met 336 and Ile 373 in ERβ (equivalent to Leu 384 and Met 421 in ERα) are positioned on opposite faces of R,R-THC (**Appendix, Figure 3b, 3c**). Modeling (based on both the THC- ERα and GEN- ERβ structures) suggests that, because of the different sizes of the side chains of these residues, the THC A' ring would have to be positioned ~ 2.4 Å lower in the ERβ binding pocket relative to its location in the crystal in order for THC to interact with Met 336 and Ile 373 and to orient His 475 and Leu 476 in productive conformations (data not shown). This lower position should be highly unfavorable because it would result in steric clashes between the B' ring ethyl group and the side chain of Leu 298 at floor of the binding pocket (**Appendix, Figure 3b, 3c**). R,R-THC presumably binds in the alternative mode observed in the crystal to avoid these steric clashes. Consistent with this hypothesis, the dimethyl analog of THC, which should be less sterically hindered from adopting the lower position, acts as a weak ERβ partial agonist (8).

Because the conformational effects of ligand binding are cooperative in nature, residues that lie outside the binding pocket may also play roles the subtype-selective effects of R,R-THC. Nevertheless, preliminary mutagenesis results indicate that Leu 384/Met 336 and Met 421/Ile 373 do contribute to these effects (**Figure 7**), at least for ERα. However, the effect is only partial for ERα and the corresponding ERβ → ERα amino acid swapping mutations (Met336 → Leu384, Ile373 → Met421) do not result in the recovery of any detectable R,R-THC agonist activity (**Figure 7B**). The same result was observed both for full length ERα and ERβ (data not shown) as well as for the LBD of each ER fused to the Gal4 DNA binding domain. In both cases, a transcriptional activation assay was used to assess ER or ER LBD activity in transiently transfected MDA-MB-231 breast cancer cells in which recombinant GRIP1 was also co-expressed (see attached manuscript for experimental details). Estradiol and OHT were tested as positive and negative controls, respectively for both ER subtypes and behaved as expected with both single and double mutations (**Figure 7A**). In total, these results indicate that the two non-conserved amino acids that line the inside of the LBD pocket (**Figure 6**) are not sufficient for selective α or β behavior in terms of response to R,R-THC. However, for other ligands, such as HPTE (**Figure 8**), these two amino acids do appear to play a major role in distinguishing between ERα and ERβ behavior (**Figure 7B**). While HPTE, an estrogenic metabolite of the organochlorine pesticide methoxychlor, is a potent ERα agonist in HepG2 cells (16), it has minimal agonist activity with either human or rat ERβ and almost completely abolishes estradiol-induced ERβ activity. Notably, exchange of the two ERα/β-distinguishing amino acids effectively converted ERα into ERβ and vice versa in a cell based reporter assay of HPTE activity (**Figure 7B, HPTE**). In contrast, the behavior of certain pyrazole derivatives, like propyl pyrazole triol (**Figures 7B and 8, PPT**), which have been shown to be selective ERα agonists with little or no affinity for ERβ (17), are unaffected by exchange of these two amino acids. The structural basis for these differences has yet to be fully determined, although significant progress has been made in the last year, as described below.

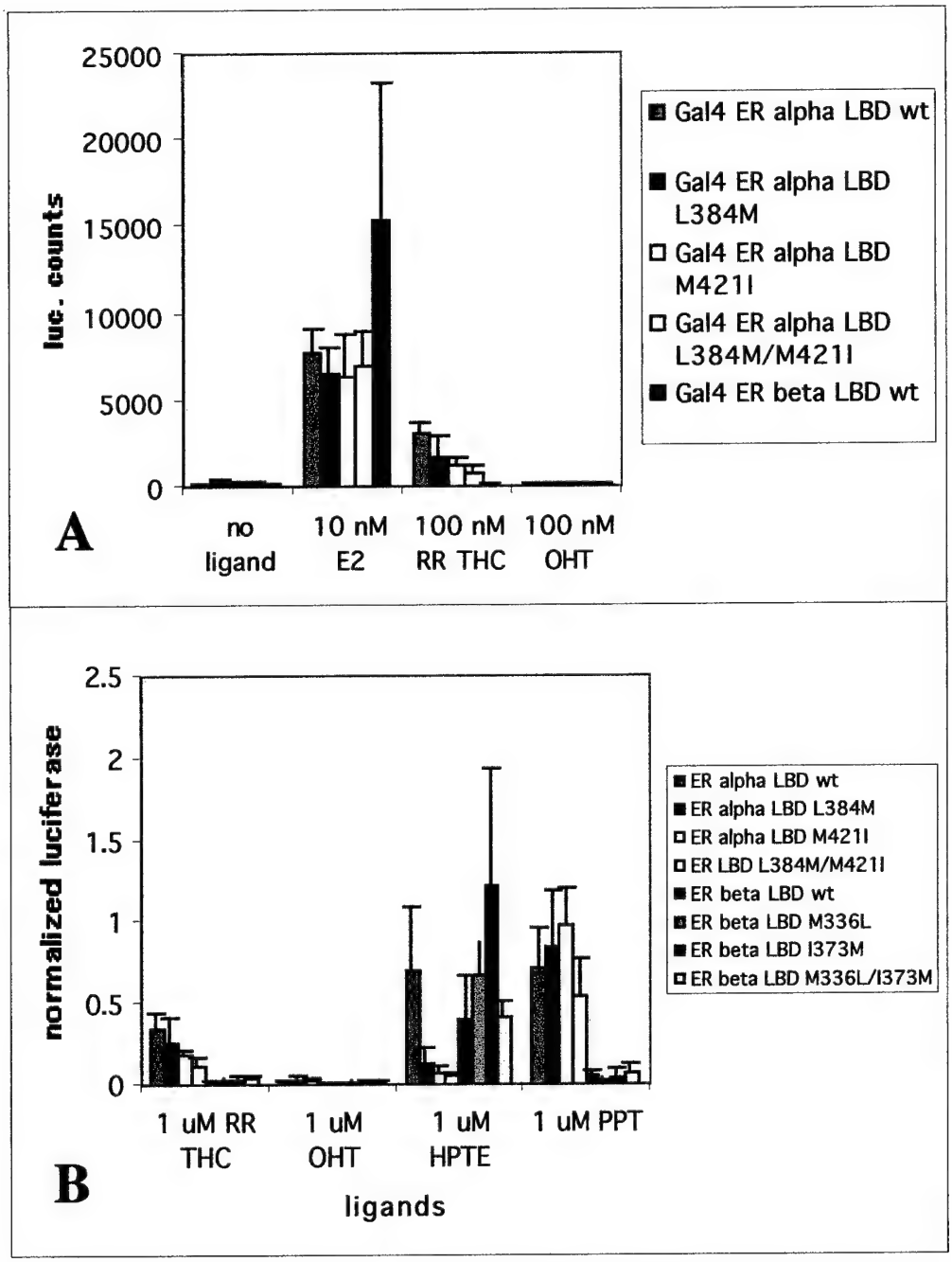

Figure 7. Transcriptional activity of Gal4-ERα/β LBD mutants versus wild type ERα/β LBDs (+ GRIP1; in MDA-MB231 cells). **A.** Positive and negative controls. **B.** ER subtype-selective ligands.

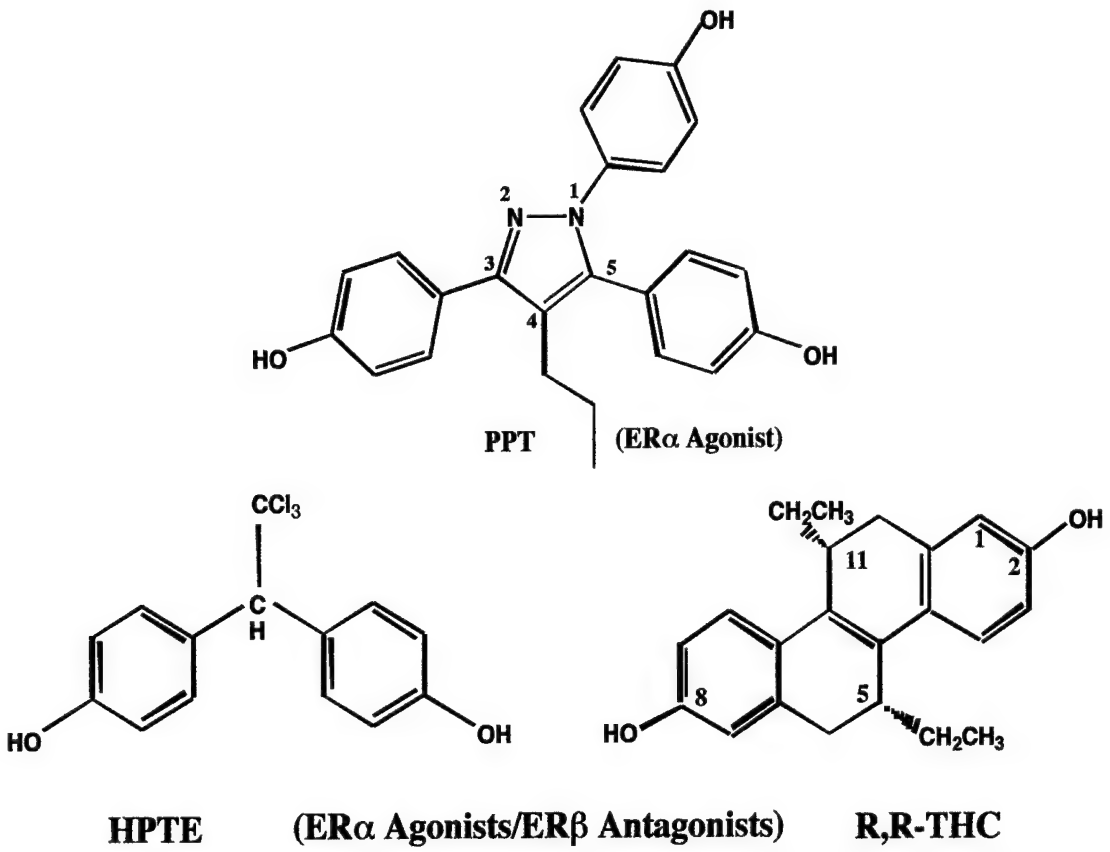

Figure 8. Structures of ERα/β subtype-selective agonists and antagonists. HPTE = *p*-hydroxyphenyl-trichloroethane. PPT = propyl pyrazole triol.

Perhaps these contrasting outcomes are not quite as surprising they appear since we and others have data to show that the two ER subtypes seem to prefer different default conformations (**Appendix, Figure 2a**) and that even for the same ER subtype, structurally similar ligands (e.g. OHT and RAL) can induce unique and subtly different conformations. Therefore, it is very likely that amino acids outside the LBD pocket contribute to ligand discrimination and ER subtype-selective behavior. Additional proof that these subtle conformational differences are real and significant comes from the development of peptides (generated by phage display) that can distinguish between complexes of ERα or ERβ bound to these ligands (18, 19). For example, a peptide designated α/β V can distinguish between the OHT-ERα/β complexes and other SERM-ER complexes, including Ral-ERα/β (18). Other peptides (e.g. 7β-16) can selectively recognize GW5638-ERα/β compared to other SERM-ER complexes (19). One of our major goals is to understand the structural/molecular basis for these differences. Thus, one approach is to determine the crystallographic structures of ERα/β LBD complexes with these ligand-selective peptides. For example, we are currently trying to crystallize GW5638-ERα LBD complexed with a peptide that only recognizes this ligand-ER complex. Interestingly, this peptide, which was identified in a phage display screen, has a high degree of homology with the nuclear receptor interaction domains (CoRNR boxes) that are present in the co-repressors N-CoR and SMRT (20).

In addition, we have and will continue to exploit site-directed mutagenesis of both ER subtypes to better define which residues distinguish ERα from ERβ in response to ligands that have unique activity- and/or ER subtype-selective behavior. An example of the value of this approach is shown in **Figure 9**. By introducing additional mutations outside the residues that line the ligand-binding pocket of ERβ LBD, we have succeeded in recovering partial response to PPT, which is a complete ERα-selective agonist. The choice of mutations was based on an analysis of differences in residue interactions between the two ER subtypes. As shown in **Figure 10**, a series of hydrogen bonds (dashed green lines) contribute to the overall structure surrounding the ligand-binding pocket of ERα. These interactions are not present in ERβ. We therefore mutated the corresponding ERβ residues to re-create these essential interactions. Interestingly, a cluster of five mutations (Mut 5) is more effective than adding two more mutations to the same cluster

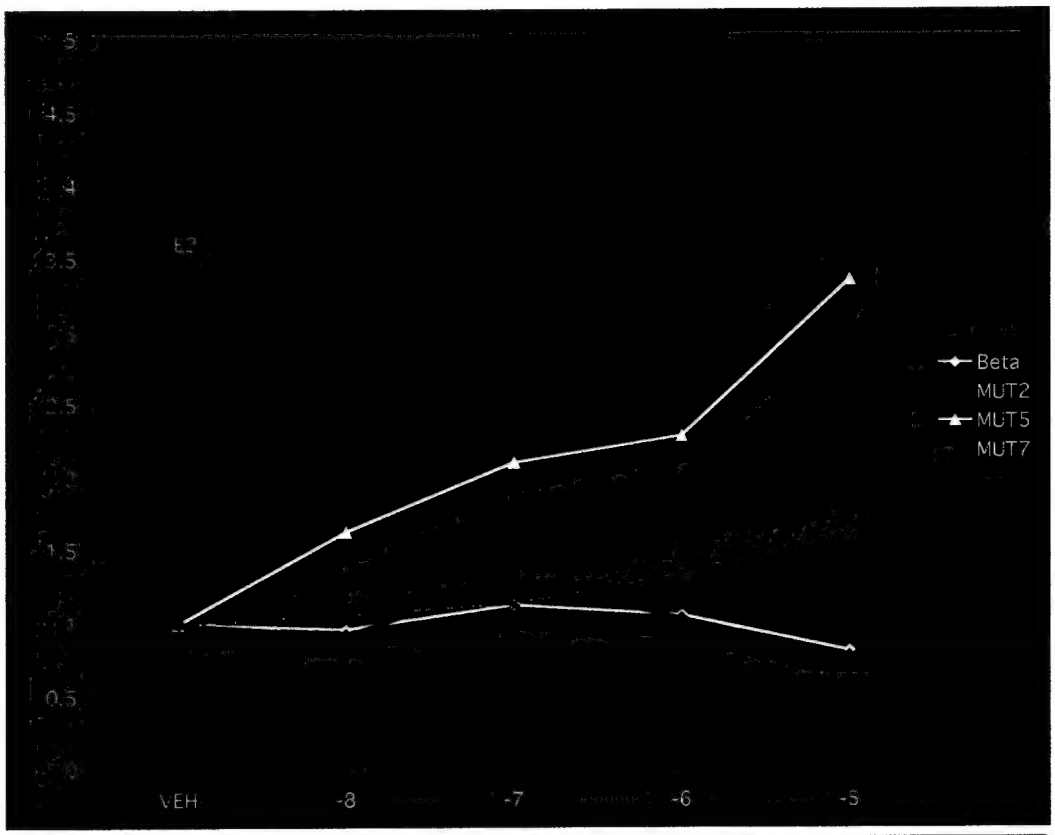

Figure 9. Transcriptional activity of ERβ mutants in response to PPT (ERE-tk-Luc; Ishikawa Cells). Dose-response curves. Beta = wild type ERβ; Mut 2 = M336L+ I373M; Mut 5 = Mut 2 + M296G + L300N + L304R; Mut 7 = Mut 5 + I282L + D359N. E2 = estradiol-mediated activity. Y axis = fold induction. X axis = log dose [ligand]. VEH = vehicle.

(Mut 7) (**Figure 9**), demonstrating that not all ERα/β residue exchanges are additive in effectiveness. The divergence of the two ER subtypes undoubtedly took a long time to evolve, which is why we are trying to use a rational structure-based approach coupled with functional assays to understand the nature of these differences. Despite considerable effort, we have yet to

determine the minimum number of residues that are required for ERβ to recognize R,R-THC as an agonist. Also, the partial recovery of PPT agonism observed in the Mut 5 ERβ (**Figure 9**) demonstrates that pocket and surface residue requirements are not the same for different ligands and the relationship between the LBDs of the two ER subtypes is more complicated than we first imagined. These data clearly illustrate that secondary structure interactions and flexibility are key determinants of ligand specificity for the two ER subtypes, revealing novel aspects of nuclear receptor function. Equally important, residues outside the ligand-binding pocket appear to be critical for ligand discrimination between two closely related nuclear receptors.

Figure 10. Hydrogen bonds that are ERα-specific. Helix 12 is shown at the far left in this partial view of the R,R-THC-ERα LBD structure. The GRIP peptide (upper left corner) is colored red.

We will continue to use a structure-based mutagenic approach to identify key residues that are responsible for ligand discrimination between the two ER subtypes. This type of information will be essential for our compound modeling and drug design efforts. We will want to know, for example, the minimum number of amino acids required for ER subtype selection for each of the compounds mentioned above. We will also need to know more about the conformational flexibility of the two ER subtypes and how that flexibility distinguishes between coactivator and corepressor preferences. The success of this project has therefore not only been very informative in its own right but has also led to new approaches that will help in the design of molecules that may have ER subtype-selective therapeutic applications in HRT and breast cancer management or prevention.

KEY RESEARCH ACCOMPLISHMENTS

- Determination and refinement of crystallographic structures of ERα and ERβ LBDs bound to R,R-THC, an ERα agonist/ERβ antagonist. New insights into mechanisms of agonism and antagonism revealed.
- Molecular basis of novel concept "passive antagonism", or antagonism without side chains, predicted from structures of ERα and ERβ LBDs bound to R,R-THC and TIF2/GRIP1 NR box II peptide.
- Novel concept of helix 12 dynamic equilibrium: Positioning of helix 12 is more variable than previously believed and is a key discriminator among diverse agonist- and antagonist-induced conformations of ERα and ERβ. Hydrophobic cleft in the LBD can accommodate coactivators (agonists), corepressors (antagonists), and/or different orientations of helix 12 in the presence of different antagonists.
- Transcriptionally active conformation of ER LBD requires cooperative participation of ligand, LBD, and coactivator.
- Molecular basis of ER subtype-selective agonism and antagonism predicted from structure of ERα and ERβ LBDs bound to R,R-THC. R,R- THC binds to the ERβ LBD without nucleating many of the equivalent cooperative interactions observed in the ERα complex that reflect agonist behavior.
- Mutagenic analysis of ERα and ERβ LBDs reveals that ligand-selective α and β character, especially transcriptional activity, depend on more than the two amino acids that differ in the ligand binding pockets of the two ERs.
- Amino acids that are required for PPT (a potent ERα-selective agonist) recognition by ERβ are identified by mutagenic analysis combined with functional assays. These resides are not sufficient for ERβ recognition of R,R-THC as an agonist.
- LBD pocket and surface residue requirements are not the same for different ligands and the relationship between the LBDs of the two ER subtypes is more complicated than first imagined. Secondary structure interactions and flexibility are key determinants of ligand specificity for the two ER subtypes, revealing novel aspects of nuclear receptor function

REPORTABLE OUTCOMES

- Manuscripts, Abstracts, Presentations:
  A manuscript detailing the results reported here was recently published in *Nature Structural Biology* (3). It is included in the Appendix.
  Abstracts for two meetings are included in the Appendix.
  Presentations:
  Seminar Speaker, Molecular and Cellular Biology Research Seminar Series, Sunnybrook and Women's College Health Sciences Centre, Toronto, Ontario, Canada, 11/01
  Symposium Speaker, Workshop on Genomic vs Non-Genomic Steroid Actions: Encountered or Unified Views, Juan March Institute, Madrid, Spain, 12/17-19, 2001.
  Symposium Speaker, Breast Cancer Symposium: Think Tank 12, St. Maarten, The Netherlands Antilles, 1/02
  Symposium Speaker, Sixth Annual Breast Cancer Symposium, Sun Valley, Idaho, 3/02
  Speaker, Sixth Annual Workshop, Frontiers in Estrogen Action, Amelia Island, FL, 4/02
- Patents: none
- Degrees obtained with award support: none

- Development of cell lines, etc: none
- Informatics:
  R,R-THC-ERα/β crystallographic coordinates have been deposited in the PDB and were released upon publication of the structures.
- Funding applied for based on work supported by this award:
  An R01 proposal (CA89489), "Development and Characterization of Novel SERMs" was funded in August, 2001. This project will continue and extend the structural work supported by this DOD award. In addition, a drug discovery project, "Development of Novel Reagents for Breast Cancer Prevention and Treatment", which complements this DOD award was funded January 1, 2002 by the Ludwig Fund for Cancer Research.
- Employment or research opportunities applied for: none

CONCLUSIONS

The major goal of this investigation was to determine the three-dimensional structures of the two known human estrogen receptors (ERα and ERβ) complexed with receptor-selective estrogens and antiestrogens (SERMs). Ligands that act differentially on ERα and ERβ are potentially valuable both as tools to dissect the biological roles of the two ERs and as novel therapeutics with pharmacological properties distinct from existing drugs. The synthetic compound, R,R-5,11-*cis*-diethyl-5,6,11,12-tetrahydrochrysene-2,8-diol (R,R-THC), was previously identified as a selective estrogen agonist when bound to ERα and as an antagonist when bound to ERβ. To better understand this selective behavior, the crystallographic structures of human ERα and ERβ ligand-binding domains (LBDs) complexed with R,R-THC were solved. Consistent with the prediction that bulky/extended side chains are not essential for antagonist behavior, R,R-THC antagonizes ERβ in a manner very different from 4-hydroxytamoxifene (OHT), raloxifene (RAL) and ICI 182,780 (ICI). The positioning of the side chains of OHT, RAL, and ICI directly or "actively" preclude the agonist-bound conformation of helix 12 by steric hindrance. Hence, we define their common mechanism of action as "active antagonism". R,R-THC does not have an extended side chain and in its complex with ERβ, helix 12 is not sterically precluded from adopting the agonist-bound conformation as it is in the other antagonist complexes. Instead, R,R-THC antagonizes ERβ by stabilizing key ligand-binding pocket residues in noninteracting conformations, and disfavoring the equilibrium to the agonist-bound conformation of helix 12. Thus, we term the mechanism of antagonism by R,R-THC as "passive antagonism". This mechanism suggests a new approach to achieving NR antagonism. Compounds could be designed to selectively stabilize the inactive conformations of certain NR subtypes and the active conformations of others, thereby eliciting novel biological and therapeutic effects.

In order to determine which amino acids are responsible for ligand discrimination between ERα and ERβ, we mutagenized the LBDs of both ERs, starting with the two residues (L384/M336, M421/I373) that differ in the pockets of each ER subtype. PPT (propyl pyrazole triol), an ERα-selective agonist with very low affinity for ERβ, as well as HPTE (2,2-bis(p-hydroxyphenyl)-1,1, 1-trichloroethane) and THC, both of which act as ERα agonists and ERβ antagonists, were used to assess the consequences of these mutations. Interestingly, conversion of the two pocket residues in ERα to the corresponding residues in ERβ markedly reduced the activity of HPTE and THC on ERα, but had no effect on PPT activity. The converse mutations in ERβ afforded

moderate agonist activity with HPTE but no activity with either PPT or THC. Thus, pocket and surface residue requirements are not the same for different ligands and the relationship between the LBDs of the two ER subtypes is more complicated than first imagined. The crystal structures of THC-ERα and ERβ LBDs suggested additional residues that might contribute to ligand selectivity through altered secondary structure interactions. Mutation of some of these residues in ERβ resulted in partial recovery of PPT agonist activity but were not sufficient to convert R,R-THC from an ERβ antagonist to an agonist. These data illustrate that secondary structure interactions and flexibility are key determinants of ligand specificity for the two ER subtypes, revealing novel aspects of nuclear receptor function. Equally important, residues outside the ligand-binding pocket appear to be critical for ligand discrimination between two closely related nuclear receptors.

So what? It is clear from the various solved structures for ERα and ERβ bound to diverse SERMs that the resulting ER conformations and ligand pharmacologies are not as simple as previously believed. Rather than just two distinct conformations of ER that reflect agonism or antagonism, it appears that multiple conformations are possible, each of which may mediate a different pharmacology for a particular ligand in a given tissue, such as the breast, uterus, bone, or cardiovascular system. It has become clear that variable antagonism can be achieved both by the presence of bulky side chains and by molecules that lack bulky side chains. Thus, it is important to solve additional structures for ERα and ERβ complexed with ligands that have been shown to have different tissue-selective pharmacologies, such as GW5638 and ICI 182,780 (Faslodex). In addition, structure-based mutagenic analyses of the two ER subtypes will help define residues that contribute to α and β activity-selective and subtype-selective behavior. Such information is essential to design compounds that have defined properties. A major goal of this investigation is to characterize and/or design compounds that are useful as chemopreventive agents, especially for breast and uterine cancers. To be useful in a clinical setting, such as hormone replacement therapy, such compounds must also have the beneficial effects of estrogen, including maintenance of bone density, protection of the cardiovasculature, prevention of hot flashes and perhaps delayed onset of Alzheimer's disease and maintenance of cognitive function. It seems unlikely that a single molecule will have all of these properties. However, it is clear that improved SERMs can be designed and/or discovered. Since most, if not all, of the behavior of the two known ERs is dictated by the conformations induced by diverse natural and synthetic ligands, determination and analysis of the corresponding 3D structures for representative SERMs should be a valuable tool for dissecting underlying molecular mechanisms and for designing new generation compounds. We will therefore continue our efforts to determine and correlate ER-SERM structures with their known biological activities and to understand the unique structural/molecular characteristics that define and differentiate ERα and ERβ. These approaches should help in the design of molecules that may have ER subtype-selective therapeutic or preventive applications in HRT, hormone/tissue-specific diseases and breast cancer.

REFERENCES

1. Shiau AK, Barstad D, Loria PM, Cheng L, Kushner PJ, Agard DA, Greene GL 1998 The structural basis of estrogen receptor/coactivator recognition and the antagonism of this interaction by tamoxifen. Cell 95:927-37

2. Pike AC, Brzozowski AM, Hubbard RE, Bonn T, Thorsell AG, Engstrom O, Ljunggren J, Gustafsson JA, Carlquist M 1999 Structure of the ligand-binding domain of oestrogen receptor beta in the presence of a partial agonist and a full antagonist. Embo J 18:4608-18
3. Shiau AK, Barstad D, Radek JT, Meyers MJ, Nettles KW, Katzenellenbogen BS, Katzenellenbogen JA, Agard DA, Greene GL 2002 Structural characterization of a subtype-selective ligand reveals a novel mode of estrogen receptor antagonism. Nat Struct Biol 9:359-64.
4. Pike AC, Brzozowski AM, Walton J, Hubbard RE, Thorsell A, Li Y, Gustafsson J, Carlquist M 2001 Structural Insights into the Mode of Action of a Pure Antiestrogen. Structure (Camb) 9:145-53.
5. Fawell SE, White R, Hoare S, Sydenham M, Page M, Parker MG 1990 Inhibition of estrogen receptor-DNA binding by the "pure" antiestrogen ICI 164,384 appears to be mediated by impaired receptor dimerization. Proc Natl Acad Sci U S A 87:6883-7.
6. Brzozowski A, Pike A, Dauter Z, Hubbard R, Bonn T, Engstrom O, Ohman L, Greene G, Gustafsson J, Carlquist M 1997 Molecular basis of agonism and antagonism in the oestrogen receptor. Nature 389:753-758
7. Barkhem T, Carlsson B, Nilsson Y, Enmark E, Gustafsson J, Nilsson S 1998 Differential response of estrogen receptor alpha and estrogen receptor beta to partial estrogen agonists/antagonists. Mol Pharmacol 54:105-12
8. Meyers MJ, Sun J, Carlson KE, Katzenellenbogen BS, Katzenellenbogen JA 1999 Estrogen receptor subtype-selective ligands: asymmetric synthesis and biological evaluation of cis- and trans-5,11-dialkyl- 5,6,11, 12- tetrahydrochrysenes. J Med Chem 42:2456-68
9. Sun J, Meyers MJ, Fink BE, Rajendran R, Katzenellenbogen JA, Katzenellenbogen BS 1999 Novel ligands that function as selective estrogens or antiestrogens for estrogen receptor-alpha or estrogen receptor-beta. Endocrinology 140:800-4
10. Schultz JR, Tu H, Luk A, Repa JJ, Medina JC, Li L, Schwendner S, Wang S, Thoolen M, Mangelsdorf DJ, Lustig KD, Shan B 2000 Role of LXRs in control of lipogenesis. Genes Dev 14:2831-8.
11. Gangloff M, Ruff M, Eiler S, Duclaud S, Wurtz JM, Moras D 2001 Crystal structure of a mutant hERalpha ligand-binding domain reveals key structural features for the mechanism of partial agonism. J Biol Chem 276:15059-65.
12. Steinmetz AC, Renaud JP, Moras D 2001 Binding of ligands and activation of transcription by nuclear receptors. Annu Rev Biophys Biomol Struct 30:329-59.
13. Singh SM, Gauthier S, Labrie F 2000 Androgen receptor antagonists (antiandrogens): structure-activity relationships. Curr Med Chem 7:211-47.
14. Greene GL, Gilna P, Waterfield M, Baker A, Hort Y, Shine J 1986 Sequence and expression of human estrogen receptor complementary DNA. Science 231:1150-4
15. Mosselman S, Polman J, Dijkema R 1996 ER beta: identification and characterization of a novel human estrogen receptor. FEBS Lett 392:49-53
16. Gaido KW, Leonard LS, Maness SC, Hall JM, McDonnell DP, Saville B, Safe S 1999 Differential interaction of the methoxychlor metabolite 2,2-bis-(p-hydroxyphenyl)-1,1,1-trichloroethane with estrogen receptors alpha and beta. Endocrinology 140:5746-53.
17. Stauffer SR, Huang Y, Coletta CJ, Tedesco R, Katzenellenbogen JA 2001 Estrogen pyrazoles: defining the pyrazole core structure and the orientation of substituents in the ligand binding pocket of the estrogen receptor. Bioorg Med Chem 9:141-50.

18. Paige LA, Christensen DJ, Gron H, Norris JD, Gottlin EB, Padilla KM, Chang CY, Ballas LM, Hamilton PT, McDonnell DP, Fowlkes DM 1999 Estrogen receptor (ER) modulators each induce distinct conformational changes in ER alpha and ER beta. Proc Natl Acad Sci U S A 96:3999-4004
19. Connor CE, Norris JD, Broadwater G, Willson TM, Gottardis MM, Dewhirst MW, McDonnell DP 2001 Circumventing tamoxifen resistance in breast cancers using antiestrogens that induce unique conformational changes in the estrogen receptor. Cancer Res 61:2917-22.
20. Xu HE, Stanley TB, Montana VG, Lambert MH, Shearer BG, Cobb JE, McKee DD, Galardi CM, Plunket KD, Nolte RT, Parks DJ, Moore JT, Kliewer SA, Willson TM, Stimmel JB 2002 Structural basis for antagonist-mediated recruitment of nuclear co-repressors by PPARalpha. Nature 415:813-7.

FINAL REPORT FOR Award Number DAMD17-99-1-9120

APPENDIX

Reprint of manuscript published in *Nature Structural Biology*:

1. Shiau AK, Barstad D, Radek JT, Meyers MJ, Nettles KW, Katzenellenbogen BS, Katzenellenbogen JA, Agard DA, Greene GL 2002 Structural characterization of a subtype-selective ligand reveals a novel mode of estrogen receptor antagonism. Nat Struct Biol 9:359-64.

Selected abstracts of presentations at national or international meetings:

1. Workshop on Genomic vs Non-Genomic Steroid Actions: Encountered or Unified Views, Juan March Institute, Madrid, Spain, 12/17-19, 2001.

2. Keystone Symposia, Nuclear Receptor Superfamily, Snowbird, Utah, $/13-19, 2002. Abstract 549

Workshop on Genomic vs Non-Genomic Steroid Actions: Encountered or Unified Views, Juan March Institute, Madrid, Spain, 12/17-19, 2001.

ERα and ERβ: Complexities of ligand recognition and its consequences

Geoffrey L. Greene. The Ben May Institute for Cancer Research, The University of Chicago, Chicago, Illinois 60637

Estrogens and SERMs (selective estrogen receptor modulators) regulate diverse cellular activities via one or both of two known estrogen receptor subtypes (ERα and ERβ) in hormone responsive tissues and cancers. Liganded ERs can interact with a complex mix of coactivators, corepressors and other signaling molecules that differ in expression and importance from tissue to tissue. In addition, different SERMs may alter the affinity and/or selectivity of one or both ERs for these coregulators, allowing for tissue selective responses. Recently, insight into the molecular basis of estrogen agonism and antagonism has been revealed by the crystal structures of ERα and ERβ ligand binding domains (LBDs) complexed with several ligands, including estradiol (E2), diethylstilbestrol (DES), raloxifene (RAL), 4-hydroxytamoxifen (OHT), and the phytoestrogen genistein (GEN). For agonists like DES, inclusion of a peptide derived from an essential LXXLL interaction motif (NR box) found in several related p160 nuclear receptor transcriptional co-activators has helped define the AF-2/co-activator interface on ER. Although agonists and antagonists bind at the same site within the core of the LBD, each induces distinct conformations in the transactivation domain (AF-2) of the LBD, especially in the positioning of helix 12, providing structural evidence for multiple mechanisms of selective antagonism in the nuclear receptor family. Interestingly, the OHT/RAL and DES/E2 structures collectively reveal and define a multipurpose docking site on ERα that can accommodate either helix 12 or one of several coregulators. In addition, a comparison of the two structures reveals that there are at least two distinct mechanisms by which structural features of OHT promote an inhibitory conformation of helix 12. Helix 12 positioning is determined both by steric considerations, such as the presence of an extended side chain in the ligand, and by local structural distortions in and around the ligand binding pocket. Thus, one would predict that effective estrogen antagonists do not necessarily require bulky or extended side chains.

Ligands that act differentially on ERα and ERβ are potentially valuable both as tools to dissect the biological roles of the two ERs and as novel therapeutics with pharmacological properties distinct from existing drugs. As part of a search for ER subtype-selective ligands, the synthetic compound, R,R-5,11-*cis*-diethyl-5,6,11,12-tetrahydrochrysene-2,8-diol (R,R-THC), was identified as a selective estrogen agonist when bound to ERα and as an antagonist when bound to ERβ. To better understand this selective behavior, the crystallographic structures of human ERα and ERβ ligand binding domains (LBDs) complexed with R,R-THC were solved and refined, suggesting mechanisms by which this compound can act as an ERα agonist and as an ERβ antagonist. Consistent with the prediction that bulky/extended side chains are not essential for antagonist behavior, R,R-THC antagonizes ERβ in a manner very different from OHT and RAL. The positioning of the side chains of OHT, RAL, and ICI directly or "actively" preclude the agonist-bound conformation of helix 12 by steric hindrance. Hence, we define their common mechanism of action as "active antagonism". R,R-THC does not have a bulky side chain and in its complex with ERβ, helix 12 is not sterically precluded from adopting the agonist-bound conformation as it is in the other antagonist complexes. Instead, R,R-THC antagonizes ERβ by stabilizing key ligand binding pocket residues in noninteracting conformations, and disfavoring the equilibrium to the agonist-bound conformation of helix 12. Thus, we term the mechanism of antagonism of R,R-THC as "passive antagonism". The passive antagonism mechanism, as revealed here through direct comparison of the two R,R-THC-ER LBD complexes, suggests a

Keystone Symposia, Nuclear Receptor Superfamily, Snowbird, Utah, $/13-19, 2002. Abstract 549

Molecular Determinants of Ligand Selectivity Between ERα and ERβ

Kendall Nettles,[+] Jim Radek,[+] Andrew Shiau,[*] John Katzenellenbogen,[°] Benita Katzenellenbogen[°] and Geoffrey Greene[+]. [+]Ben May Institute for Cancer Research, University of Chicago, Chicago, IL; [*]Tularik Inc., South San Francisco, CA; [°]Dept. of Chemistry and Dept. of Molecular and Integrative Physiology, University of Illinois at Urbana, Urbana IL.

The development of ligands that are selective for ERα or ERβ provides an important tool for dissecting their different roles *in vivo*, and for understanding the structural basis of their ER subtype selectivity. In order to delineate which amino acids determine ligand selectivity, we undertook a mutational analysis within the ligand-binding domains of the full-length estrogen receptors, starting with the two residues (L384/M336, M421/I373) that differ in the ligand-binding pockets of each ER subtype. We examined PPT (propyl pyrazole triol), an ERα-selective agonist with very low affinity for ERβ, as well as HPTE (2,2-bis(p-hydroxyphenyl)-1,1, 1-trichloroethane) and THC (R,R-5,11-*cis*-diethyl-5,6,11,12- tetrahydro-chrysene-2,8-diol), which act as agonists on ERα but as antagonists on ERβ. Mutation of the two ligand-binding pocket residues in ERα to the corresponding residues in ERβ reduced the activity of HPTE and THC on ERα, but had no effect on PPT activity. The converse mutations in ERβ produced moderate agonist activity only with HPTE. The recently solved crystal structures of THC bound to the ERα and ERβ LBDs suggested additional residues on the surface that might contribute to ligand selectivity through altered secondary structure interactions. THC does not enter into the pocket as deeply in ERβ as in ERα, which results in a flexing of helix 11 away from the pocket to accommodate the ligand. Both the flexibility of helix 11 and the position of helix 12 can be explained by amino acid differences in helix 3. ERα Gly 344 and Asn 348 stabilize the agonist position by interacting with the loop between helix 11 and 12, and forming a hydrogen bond with the beginning of helix 12, respectively. The corresponding ERβ Met 296 and Lys 300 residues do not promote these agonist stabilizing interactions, suggesting that helix 12 may be preferentially positioned away from helix 11 to allow greater flexibility in accommodating ligands. This flexibility is needed because the back of the ligand pocket appears to be narrower in ERβ. The distance between the beta sheet and helix 3 is linked with six additional hydrogen bonds in ERα that are not present in ERβ, associated with residues Ser329, Asn352, and Asn407. Mutational analysis revealed that PPT and HPTE act as partial agonists on ERβ after mutating the ligand pocket and surface residues described above to the corresponding residues in ERα. HPTE displayed less agonist activity with the ligand pocket mutants alone. In contrast, additional mutations appear to be required for ERβ to recognize PPT as an agonist, suggesting that ligands differ in the relative contributions that ligand pocket and surface residues make in determining receptor activity. This work illustrates that secondary structure interactions and flexibility are key determinants of ligand specificity for the two ER subtypes, revealing novel aspects of nuclear receptor function. Equally important, this may be the first example of nuclear receptor subtype specificity with determinants outside the ligand-binding pocket.

1) Kendall Nettles
2) 773-702-6966 or -6964
3) Nuclear Receptor Superfamily (D4)
4) Workshop 1: Hot Topics and/or Presentations by Young Investigators.

We have several movies to illustrate the molecular details of the crystallographic analysis.

Structural characterization of a subtype-selective ligand reveals a novel mode of estrogen receptor antagonism

Andrew K. Shiau[1,2], Danielle Barstad[3], James T. Radek[3], Marvin J. Meyers[4], Kendall W. Nettles[3], Benita S. Katzenellenbogen[5], John A. Katzenellenbogen[4], David A. Agard[1] and Geoffrey L. Greene[3]

[1]The Howard Hughes Medical Institute and Department of Biochemistry and Biophysics, University of California, San Francisco, California 94143, USA. [2]Tularik Inc., Two Corporate Drive, South San Francisco, California 94080, USA. [3]The Ben May Institute for Cancer Research and Department of Biochemistry and Molecular Biology, University of Chicago, Chicago, Illinois 60637, USA. [4]Department of Chemistry, University of Illinois, Urbana, Illinois 61801, USA. [5]Departments of Molecular and Integrative Physiology and Cell and Structural Biology, University of Illinois, Urbana, Illinois 61801, USA

Published online: 15 April 2002, DOI: 10.1038/nsb787

The R,R enantiomer of 5,11-cis-diethyl-5,6,11,12-tetrahydrochrysene-2,8-diol (THC) exerts opposite effects on the transcriptional activity of the two estrogen receptor (ER) subtypes, ERα and ERβ. THC acts as an ERα agonist and as an ERβ antagonist. We have determined the crystal structures of the ERα ligand binding domain (LBD) bound to both THC and a fragment of the transcriptional coactivator GRIP1, and the ERβ LBD bound to THC. THC stabilizes a conformation of the ERα LBD that permits coactivator association and a conformation of the ERβ LBD that prevents coactivator association. A comparison of the two structures, taken together with functional data, reveals that THC does not act on ERβ through the same mechanisms used by other known ER antagonists. Instead, THC antagonizes ERβ through a novel mechanism we term 'passive antagonism'.

The physiological effects of both endogenous and synthetic estrogens are mediated by the estrogen receptors (ERs), ERα and ERβ, which are members of the nuclear receptor (NR) superfamily of ligand-regulated transcription factors[1,2]. In a search for ER subtype-selective ligands, the *R,R* enantiomer of 5,11-*cis*-diethyl-5,6,11,12-tetrahydrochrysene-2,8-diol (THC) (Fig. 1*a*) was determined to be a novel ER ligand, with an approximate six-fold affinity preference for ERβ over ERα and profoundly different activation profiles on the two ERs[3,4]. THC functions as an agonist on ERα, with an EC_{50} of ~3 nM, but has no effect on the transcriptional activity of ERβ. Instead, this compound potently antagonizes the effects of the endogenous estrogen 17β-estradiol (E2) on ERβ, with an $IC_{50} < 10$ nM. Consistent with these subtype-specific effects on transcriptional activation, THC also affects the two ERs differently in protease protection and other biochemical assays[5].

The C-terminal ligand-binding domains (LBDs) of ERα and ERβ each contain a ligand-responsive transcriptional activation function (AF-2)[6–9]. Agonists, such as E2 and diethylstilbestrol (DES), increase AF-2 activity. In contrast, pure antagonists, such as ICI 164,384 (ICI), and mixed-function partial agonist/antagonists, such as 4-hydroxytamoxifen (OHT) and raloxifene (RAL), block AF-2 activity[10–12] (Fig. 1*a*). The effects of THC on the transcriptional activity of fusions between the GAL4 DNA-binding domain and the two ER LBDs indicate that THC stimulates ERα AF-2 activity and inhibits agonist-induced ERβ AF-2 activity (data not shown), consistent with its effects on the full-length receptors.

Structural studies indicate that NR ligands regulate AF-2 activity by modulating the structure of NR LBDs[13,14]. NR ligands bind to their cognate receptors within a hydrophobic pocket formed within the core of the narrower or 'lower' half of the LBD. The binding of an agonist to an NR LBD stabilizes the positioning of the most C-terminal helix of the LBD, helix 12, such that it lies across the opening to the binding pocket formed by

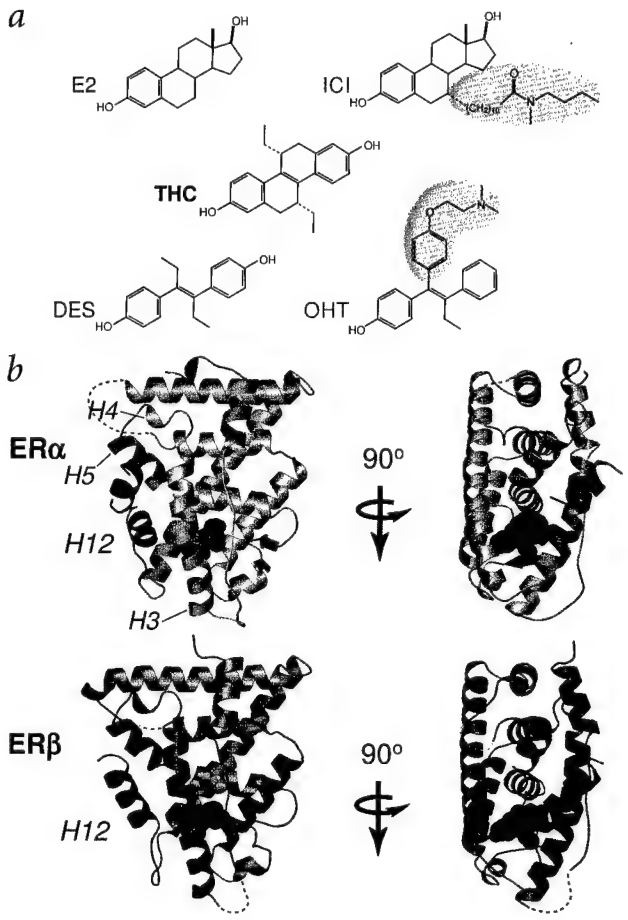

Fig. 1 Overall structures of the THC–ER LBD complexes. ***a***, Chemical structures of 17β-estradiol (E2), ICI 164,384 (ICI), diethylstilbestrol (DES), 4-hydroxytamoxifen (OHT) and *R,R*-5,11-*cis*-diethyl-5,6,11,12-tetrahydrochrysene-2,8-diol (THC). The side chains of ICI and OHT are highlighted in orange. ***b***, Two equivalent orthogonal views of the THC–ERα LBD–GRIP1 NR box II peptide and the THC–ERβ LBD complexes, showing that the two ER LBDs adopt distinct conformations when bound to THC. Both the ERα and ERβ LBDs are depicted in ribbon representation and colored light green and blue, respectively. In both complexes, helix 12 is colored red, and THC (green) is shown in space-filling representation. In the ERα complex, the coactivator peptide is depicted as a purple ribbon, and helices 3, 4, 5 and 12 have been labeled H3, H4, H5, and H12. Dashed lines represent regions of the structures that have not been modeled. Panel (*b*) and Figs 2*a*, 3*a,c* and 4 were generated using BOBSCRIPT[32] and rendered using Raster3D[33].

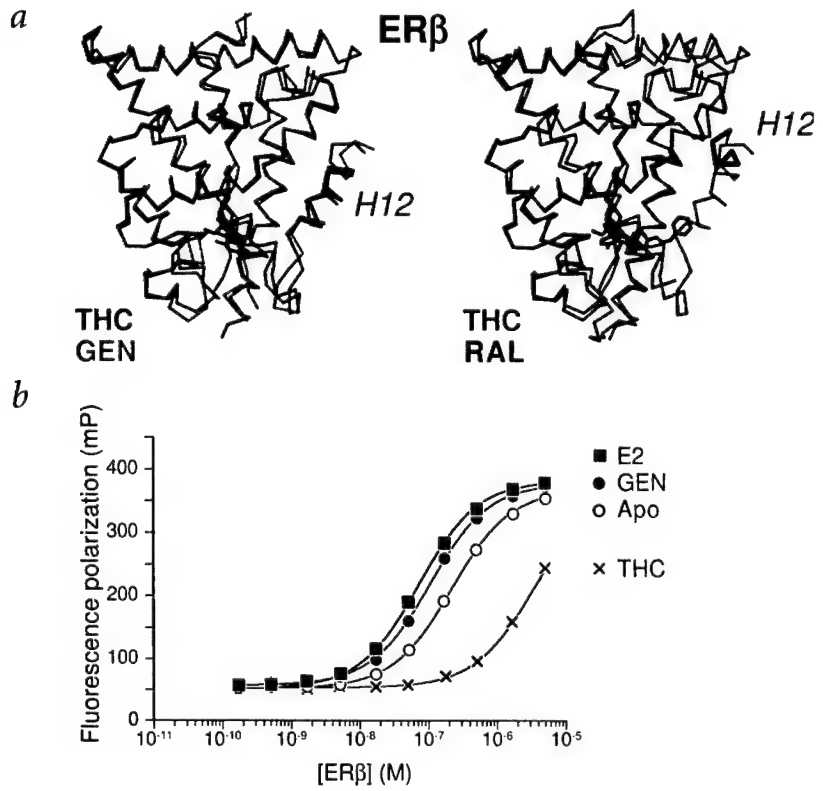

Fig. 2 Conformational equilibrium of helix 12. ***a***, Superpositions of the Cα trace of the THC–ERβ LBD complex (light blue) on those of the GEN–ERβ LBD (yellow) and the RAL–ERβ LBD (orange) complexes. Helix 12 in the RAL and GEN structures is colored red. Least squares superpositions were generated using LSQMAN[34] (THC/RAL has 1.0 Å r.m.s. deviation over 196 matched atoms with a 3.8 Å cutoff, and THC/GEN has 1.1 Å r.m.s. deviation over 218 matched atoms with a 3.8 Å cutoff). Helix 12 from each of the monomers in the THC–ERβ, GEN–ERβ and THC–ERα crystals is located in a distinct packing environment, indicating that the similarities/differences in helix 12 positioning among these complexes are not the consequence of crystal lattice effects. ***b***, Equilibrium binding of a rhodamine-labeled Leu-X-X-Leu-Leu motif-containing peptide to the ERβ LBD alone or bound to E2, DES, GEN and THC was analyzed by measuring fluorescence polarization as a function of receptor or ligand–receptor complex concentration. Values represent the mean ± s.d. for each experimental condition performed in triplicate, and the data were fit using nonlinear least squares analysis (K_d[E2] = 71 ± 2 nM, K_d[GEN] = 104 ± 4 nM, K_d[apo] = 215 ± 5 nM and K_d[THC] = 3.3 ± 0.3 μM).

helices 3, 5/6 and 11. This conformation of the LBD allows the receptor to interact with a class of proteins known as transcriptional coactivators, which mediate ligand-dependent transcription of NRs[15]. p160 coactivators recognize agonist-bound NR LBDs *via* the short sequence motif, Leu-X-X-Leu-Leu (where X is any amino acid), called the NR box[15]. NR boxes form amphipathic α-helices that recognize a hydrophobic groove on the surface of an agonist-bound LBD formed by residues from helices 3, 4, 5 and 12 (ref. 13). NR AF-2 antagonists sterically preclude the proper formation of the NR box-binding site[13,14]. The structures of the BMS614–retinoic acid receptor-α[16], OHT–ERα[17], RAL–ERα[18], RAL–ERβ[19] and ICI–ERβ[20] LBD complexes reveal that each of these antagonists possesses a bulky side chain (Fig. 1*a*) that cannot be contained within the ligand binding pocket. These side chains protrude out of the opening to the binding pocket formed by helices 3, 5/6 and 11, thereby preventing helix 12 from adopting the agonist-bound conformation. The positioning of the side chains of BMS614, OHT and RAL forces helix 12 to adopt an alternative conformation in which it binds to and occludes the remainder of the coactivator binding site by mimicking the interactions formed by the NR box[16–19]. The ICI side chain, in contrast, binds directly to the coactivator-binding site of ERβ, causing helix 12 to be completely disordered[20]. The structure of the ERβ LBD bound to the ERβ partial agonist genistein (GEN) reveals that ligand binding can stabilize yet another conformation of helix 12 (ref. 19). In this complex, helix 12 is bound over the ligand-binding pocket in a position such that it occludes the coactivator recognition surface only partially. However, the functional significance of this conformation of the LBD is unclear.

Given its behavior in transactivation and other assays[3–5], THC would be predicted to both stabilize a conformation of the ERα LBD that favors coactivator binding and one of the ERβ LBD that precludes coactivator binding. However, because it lacks a bulky side chain similar to those of OHT, RAL and ICI, THC must antagonize ERβ through a fundamentally different mechanism (Fig. 1*a*). Here we describe structural and additional functional characterization of the effects of THC on ERα and ERβ. These studies indicate that THC exerts its effects on the AF-2 activity of the two ERs by stabilizing distinct conformations of the two receptors and that THC antagonizes ERβ through a novel mechanism we term 'passive antagonism'.

Structures of the THC–ER LBD complexes

Crystals of ERα LBD bound to both THC and a peptide containing the second NR box of the p160 coactivator GRIP1 (ref. 15), and the ERβ LBD bound to THC were grown. Both structures were determined by molecular replacement. The ERα complex structure has been refined to an R-factor of 20.3% (R_{free} = 24.3%) using data to 1.95 Å, and the ERβ complex structure has been refined to an R-factor of 25.9% (R_{free} = 29.9%) using data to 2.95 Å (Table 1; Figs 1*b*, 3*a*).

As anticipated, the ERα LBD when bound to THC adopts the same conformation as it does when bound to the full agonists E2 and DES[17,18] (Fig. 1*b*). Helix 12 adopts the agonist-bound conformation, which promotes NR box association. In contrast, the binding of THC to ERβ LBD does not stabilize the agonist-bound conformation of helix 12 (Fig. 1*b*). Surprisingly, helix 12 does not bind to the region of the coactivator recognition groove formed by helices 3, 4 and 5 as it does in the OHT–ERα, RAL–ERα and RAL–ERβ complexes, and it is not disordered as it is in the ICI–ERβ complex (Fig. 2*a*). Instead, helix 12 in the THC–ERβ complex adopts an orientation most similar to that observed in the GEN–ERβ complex (Fig. 2*a*). In both complexes, helix 12 is stabilized in this conformation by hydrophobic contacts formed by Val 487, Leu 491, Met 494 and Leu 495 with the rest of the LBD[19] (data not shown).

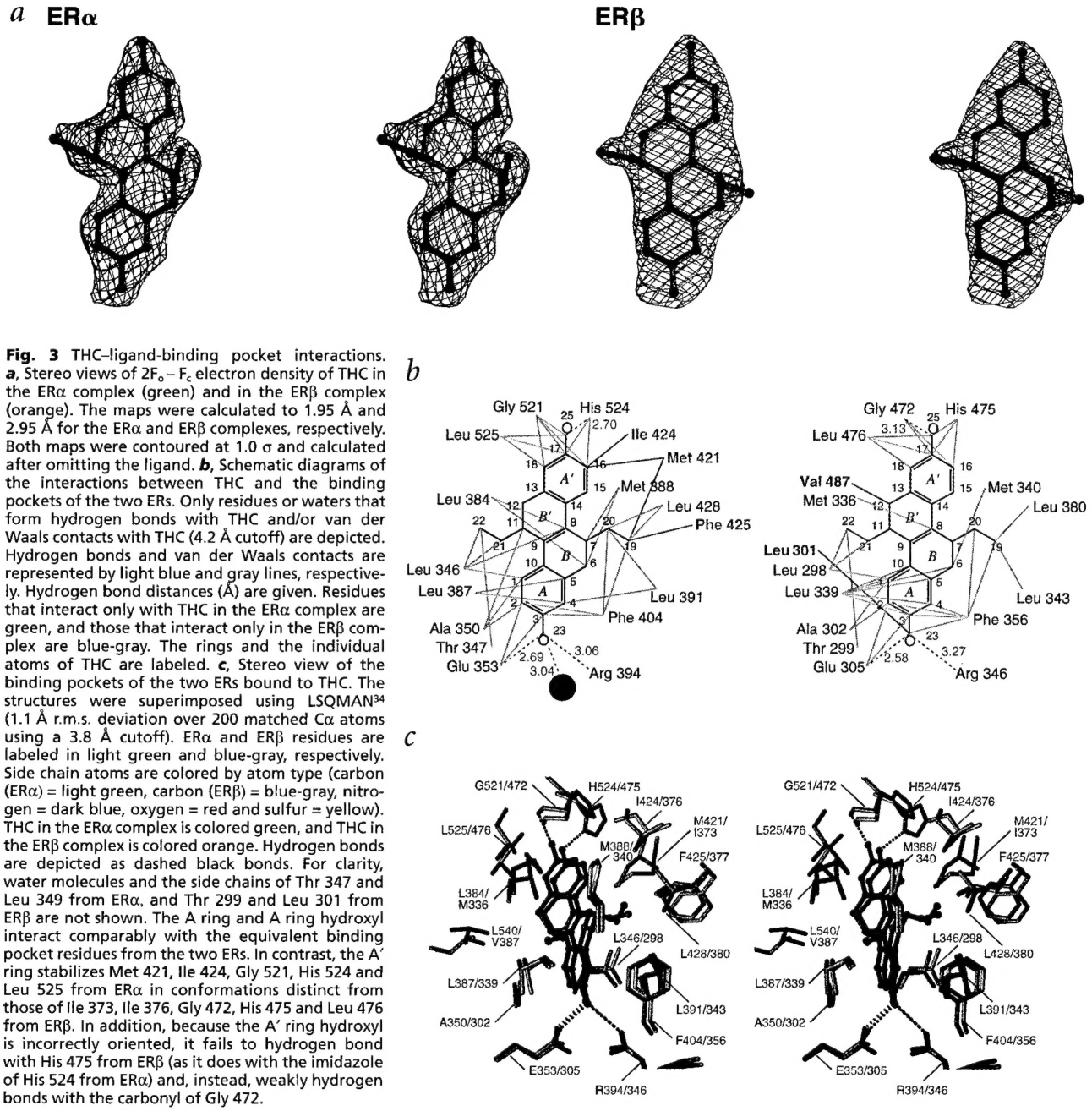

Fig. 3 THC–ligand-binding pocket interactions. ***a***, Stereo views of $2F_o - F_c$ electron density of THC in the ERα complex (green) and in the ERβ complex (orange). The maps were calculated to 1.95 Å and 2.95 Å for the ERα and ERβ complexes, respectively. Both maps were contoured at 1.0 σ and calculated after omitting the ligand. ***b***, Schematic diagrams of the interactions between THC and the binding pockets of the two ERs. Only residues or waters that form hydrogen bonds with THC and/or van der Waals contacts with THC (4.2 Å cutoff) are depicted. Hydrogen bonds and van der Waals contacts are represented by light blue and gray lines, respectively. Hydrogen bond distances (Å) are given. Residues that interact only with THC in the ERα complex are green, and those that interact only in the ERβ complex are blue-gray. The rings and the individual atoms of THC are labeled. ***c***, Stereo view of the binding pockets of the two ERs bound to THC. The structures were superimposed using LSQMAN[34] (1.1 Å r.m.s. deviation over 200 matched Cα atoms using a 3.8 Å cutoff). ERα and ERβ residues are labeled in light green and blue-gray, respectively. Side chain atoms are colored by atom type (carbon (ERα) = light green, carbon (ERβ) = blue-gray, nitrogen = dark blue, oxygen = red and sulfur = yellow). THC in the ERα complex is colored green, and THC in the ERβ complex is colored orange. Hydrogen bonds are depicted as dashed black bonds. For clarity, water molecules and the side chains of Thr 347 and Leu 349 from ERα, and Thr 299 and Leu 301 from ERβ are not shown. The A ring and A ring hydroxyl interact comparably with the equivalent binding pocket residues from the two ERs. In contrast, the A′ ring stabilizes Met 421, Ile 424, Gly 521, His 524 and Leu 525 from ERα in conformations distinct from those of Ile 373, Ile 376, Gly 472, His 475 and Leu 476 from ERβ. In addition, because the A′ ring hydroxyl is incorrectly oriented, it fails to hydrogen bond with His 475 from ERβ (as it does with the imidazole of His 524 from ERα) and, instead, weakly hydrogen bonds with the carbonyl of Gly 472.

Ligands and helix 12 positioning

Based on the position of helix 12, the ERβ LBD in the conformation stabilized by THC and GEN should be incapable of interacting with coactivators and, hence, transcriptionally silent[19]. However, GEN and THC clearly show different activities on ERβ in mammalian cells: GEN is a partial agonist[9] and THC is a pure antagonist[3,4]. How can the structural data be reconciled with the different activities of these compounds in transcriptional assays?

The simplest model that explains these data is based on two hypotheses. First, helix 12 in the unliganded ERβ LBD is in equilibrium between the inactive conformation observed in the THC– and GEN–ERβ LBD structures and the active agonist-bound conformation. Second, rather than inducing a single static conformation of helix 12, ligands affect LBD transcriptional activity by shifting this equilibrium. As a consequence, helix 12 in the unliganded or apo ERβ LBD, although largely in a transcriptionally silent conformation, may also adopt a transcriptionally active one. Hence, the low but detectable constitutive AF-2-derived transcriptional activity of the unliganded receptor[9] results from the modest but significant ability of the apo LBD to bind coactivator. Full agonists, such as E2 and DES, shift the helix 12 conformational equilibrium in favor of the active conformation and stimulate AF-2 activity by increasing the affinity of the LBD for coactivator. Because partial agonists, such as GEN, are incapable of shifting the equilibrium in favor of the active conformation to the same extent as full agonists, they are able only to incrementally increase the affinity of the receptor for coactivator and, hence, activate AF-2 less efficiently than full

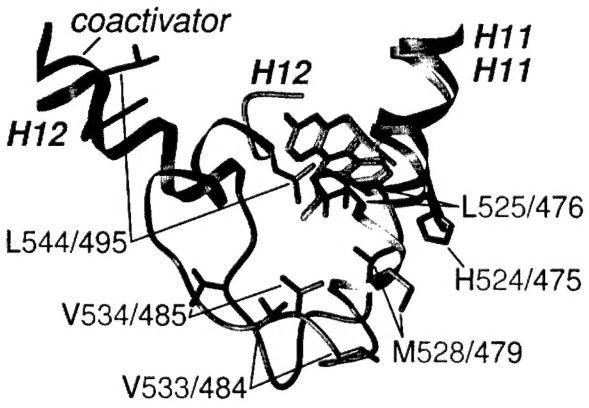

Fig. 4 Ligand-binding pocket residues influence helix 12 positioning. The structures of the two complexes were superimposed, and the side chains and ligands are colored as in Fig. 3c. In addition, the peptide backbone of ERα, ERβ and the coactivator peptide are colored light green, blue-gray and purple, respectively. In each structure, helices 11 and 12 are labeled H11 and H12, and, for clarity, the ligands have been made semi-transparent. The side chain of Met 479 from ERβ is disordered and depicted as an Ala residue. In the ERα complex, His 524, Leu 525 and Met 528 are oriented by the THC A′ ring such that they can form nonpolar contacts with residues from helix 12 or the preceding loop (Val 533, Val 534 and Leu 544). Because of the distinct positioning of His 475 and Leu 476 (His 524 and Leu 525 in ERα) stabilized by the A′ ring, the equivalent interactions do not occur in the ERβ complex.

agonists. GEN binding should permit the ERβ LBD to sample both inactive and active conformations of helix 12 (possibly to comparable extents). The observation of the inactive conformation in the GEN complex structure may reflect the true bias of the equilibrium in solution or it may result from the influence of the crystallization conditions on the equilibrium.

In principle, THC could antagonize receptor activity by shifting the equilibrium to favor the inactive THC/GEN-bound conformation. If THC binding forces the receptor to sample this conformation more than it does in the absence of ligand, the THC–receptor complex would be expected to have an even lower affinity for coactivator than the unliganded receptor. This would agree with the absence of transcriptional activity of the THC–ERβ complex and the conformation of helix 12 observed in the crystal.

The helix 12 conformational equilibrium would be difficult to observe directly. Nonetheless, the predicted actions of the various ligands, inferred from the model described above, suggest a testable hypothesis. The binding of different ligands should modulate the affinity of the ERβ LBD for coactivator such that E2–LBD > GEN–LBD > apo LBD > THC–LBD. The affinities of various ligand–ERβ LBD complexes for an Leu-X-X-Leu-Leu motif-containing peptide were directly measured using a fluorescence polarization-based binding assay[21], and the expected rank order of affinities was observed for the different complexes (Fig. 2*b*). Thus, these and other biochemical data[5] suggest that helix 12 positioning in ERβ, as in the case of other NRs[13], is dictated by a ligand-sensitive conformational equilibrium.

THC–ligand binding pocket interactions

When ER agonists bind to ERα (and presumably ERβ), they favor the active conformation of helix 12 but they do so indirectly. These ligands form hydrogen bonds and van der Waals contacts with residues from helices 3, 6, 8 and 11 and the β-hairpin, positioning these residues in conformations that allow their interaction with each other and with neighboring residues surrounding the binding pocket. The formation of these cooperative interactions positions residues from helices 3, 5 and 11 such that they create a predominantly hydrophobic binding surface for the loop connecting helices 11 and 12 and helix 12 itself[17,18].

THC interacts with the ERα LBD similar to the full agonists, DES and E2, and nucleates all of the polar and nonpolar interactions required to favor the positioning of helix 12 in the agonist-bound conformation[17,18] (Fig. 3*b*,*c*). For example, in the ERα complex, the A′ ring forms hydrogen bonds and/or nonpolar contacts with the side chains of His 524 and Leu 525 (Fig. 3*b*,*c*), stabilizing them in conformations such that they form (either directly or indirectly) part of the binding site for helix 12 or the preceding loop. The side chain of His 524 forms hydrophobic contacts with the side chain of Met 528, positioning it such that it can, in turn, form nonpolar contacts with the side chains of Val 533 and Val 534 from the loop between helices 11 and 12 (Fig. 4). The side chain of Leu 525 packs against that of Leu 544 from helix 12 (Fig. 4).

Although it binds to ERβ in a similar overall manner, THC fails to stabilize many of the interactions in the A′ ring region of the binding pocket that were observed in the ERα complex (Fig. 3*b*,*c*). In the ERβ complex, the B-ring ethyl group adopts a more extended conformation than in the ERα complex, causing the tetrahydrochrysene scaffold to be tilted by 5° towards the opening formed by helices 3, 5 6 and 11, and away from the floor of the binding pocket. Because the A′ ring is displaced by ~0.7 Å from its position in the ERα complex (Fig. 3*c*), the side chains of His 475 and Leu 476 (which form only nonpolar contacts with the A′ ring) are positioned ~1.6 and 2.3 Å away, respectively, from the locations of their counterparts in the ERα complex (His 524 and Leu 525) (Figs 3*c*, 4). As a result, the side chain of His 475 fails to pack against that of Met 479 (equivalent to Met 528 in ERα), causing the Met 479 side chain to be disordered. The backbone atoms of Met 479 and the residues flanking it adopt a random coil conformation (as compared to the helical conformation adopted by their counterparts in ERα), and Met 479 is located 2.4 Å distant from Met 528 (based on Cα atoms) (Fig. 4). Consequently, both Leu 476 and Met 479 are not positioned appropriately to form interactions with relevant residues from helix 12 and the preceding loop (Val 484, Val 485 and Leu 495) that would stabilize the active conformation of helix 12 (Fig. 4). Therefore, these residues destabilize the active conformation of helix 12 (Fig. 4). Thus, by positioning certain binding pocket residues in nonproductive conformations, the binding of THC to ERβ disfavors the agonist-bound conformation of helix 12 and shifts the equilibrium towards the inactive conformation of helix 12.

The two ligand-binding pocket residues that differ between the two subtypes may explain the failure of THC to act as an ERβ agonist. Met 336 and Ile 373 in ERβ (equivalent to Leu 384 and Met 421 in ERα) are positioned on opposite faces of THC (Fig. 3*b*,*c*). Modeling (based on both the THC–ERα and GEN–ERβ structures) suggests that the THC A′ ring would have to be positioned ~2.4 Å lower in the ERβ binding pocket relative to its location in the crystal in order for THC to both interact with Met 336 and Ile 373 and orient His 475 and Leu 476 in productive conformations (data not shown). This lower position should be highly unfavorable because it would result in steric clashes between the B′ ring ethyl group and the side chain of

Table 1 Summary of Crystallographic Statistics

Data collection		
Complex	THC–ERα LBD–GRIP1 NR Box II peptide	THC–ERβ LBD
Space group	$P2_1$	R3
Resolution (Å)[1]	1.95 (2.02–1.95)	2.95 (3.06–2.95)
Observations		
Total	119,409	64,540
Unique	34,533	14,895
Completeness (%)[1]	97.9 (97.7)	99.7 (100)
R_{sym} (%)[1,2]	6.5 (53.1)	4.5 (30.2)
$\langle I \rangle / \langle \sigma (I) \rangle$[1]	18.8 (2.9)	23.3 (3.4)
Refinement		
Number of atoms		
Protein	3,830	3,409
Water	166	9
Heterogen	53	48
R_{cryst} (%)[1,3]	20.3 (29.6)	25.9 (34.0)
R_{free} (%)[1,3]	24.3 (33.6)	29.9 (35.1)
R.m.s. deviation		
Bonds (Å)	0.005	0.011
Angles (°)	1.08	1.29
Average B-factor (Å^2)	38.5	40.1

[1]Values in parentheses refer to the highest resolution shell.
[2]$R_{sym} = \Sigma|I_h - \langle I_h \rangle| / \Sigma I_h$, where I_h is the integrated intensity of a given reflection and $\langle I_h \rangle$ is the average intensity over symmetry equivalents.
[3]$R_{cryst} = \Sigma||F_o| - |F_c|| / \Sigma|F_o|$, where F_o and F_c are observed and calculated amplitudes, respectively. R_{free} is calculated similarly using a test set of reflections.

Leu 298 at floor of the binding pocket (Fig. 3*b*,*c*). THC presumably binds in the alternative mode observed in the crystal to avoid these steric clashes. Consistent with this, the dimethyl analog of THC, which should be less sterically hindered from adopting the lower position, acts as a weak ERβ partial agonist[3].

Antagonism without a side chain

Because the positioning of the side chains of OHT, RAL and ICI directly or 'actively' precludes the agonist-bound conformation of helix 12 by steric hindrance[13,14], we term their common mechanism of action as 'active antagonism'. Clearly, THC lacks a bulky side chain, and in its complex with ERβ, helix 12 is not sterically precluded from adopting the agonist-bound conformation (Fig. 4). Instead, THC antagonizes ERβ by stabilizing nonproductive conformations of key residues in the ligand-binding pocket, thereby disfavoring the equilibrium to the agonist-bound conformation of helix 12 and leading to stabilization of an inactive conformation of helix 12. Thus, we call the mechanism of antagonism of THC 'passive antagonism'.

Passive antagonism may not be unique to THC and ERβ. There are many examples of NR ligands that act as antagonists even though they are smaller than the endogenous agonists of these NRs. The synthetic androgen receptor antagonist, flutamide, is comparable in size to testosterone and does not possess an obvious moiety that would act as an antagonist side chain[22]. Similarly, progesterone is smaller than aldosterone but is a high affinity antagonist of the mineralocorticoid receptor[23].

Many NRs have several subtypes that possess distinct expression patterns and regulate distinct target genes[24]. Antagonists generated through the addition of bulky side chains to agonist scaffolds are limited to being antagonistic on one or more subtypes of a particular NR[13,14]. The passive antagonism mechanism, as revealed here through direct comparison of the two THC–ER LBD complexes, suggests a new approach to achieving NR antagonism. Compounds could be designed to selectively stabilize the inactive conformations of certain NR subtypes and the active conformations of others. Such ligands may exert novel biological and therapeutic effects.

Methods

Protein expression and purification. The human ERα LBD (residues 297–554) was expressed, carboxymethylated and purified as described[17]. For crystallographic studies, the human ERβ LBD (residues 256–505) was expressed as an N-terminally His_6-tagged fusion protein in BL21(DE3)pLysS cells using a modified pET-15b plasmid (Novagen). Bacterial lysates were applied to an estradiol-Sepharose column, and the bound ERβ LBD was carboxymethylated with 20 mM iodoacetic acid. Protein was eluted with 30 μM THC in ~50 ml of 20 mM Tris-HCl, 1 M urea and 10% (v/v) dimethyl formamide (DMF), pH 8.1. The ERβ LBD was further purified by ion exchange chromatography (Resource Q, Pharmacia). Protein samples were analyzed by SDS-PAGE, native PAGE and electrospray ionization mass spectrometry. For biochemical studies, residues 214–530 of human ERβ were expressed as a fusion with glutathione-S-transferase (GST) in BL21 cells using a modified pGEX-4T1 plasmid (Pharmacia). The GST fusion protein was bound to glutathione Sepharose 4 Fast Flow (Pharmacia) and eluted with glutathione per the manufacturer instructions. In some experiments, the protein was further purified by ion exchange chromatography (HiTrap Q, Pharmacia).

Crystallization and data collection. Crystals of the THC–ERα LBD–GRIP1 NR box II peptide complex were prepared by hanging drop vapor diffusion at 19–21 °C. Before crystallization, the THC–ERα LBD complex was incubated overnight with a four-fold molar excess of the GRIP1 NR box II peptide. Samples (0.5 μl) of this solution (5.0 mg ml^{-1} protein) were mixed with 3.5 μl of reservoir buffer consisting of 16% (w/v) PEG 4000, 53 mM Tris-HCl, pH 8.8, and 50 mM $MgCl_2$ and suspended over wells containing 800 μl of the reservoir buffer. The crystals lie in the spacegroup $P2_1$, with cell dimensions a = 54.55 Å, b = 82.60 Å, c = 59.04 Å and β = 111.53°. Two independent THC-LBD–peptide complexes form the asymmetric unit. A crystal was transferred to a cryo-solvent solution containing 20% (w/v) PEG 4000, 15% (v/v) ethylene glycol, 100 mM Tris-HCl, pH 8.6, and 100 mM $MgCl_2$ and frozen in an N_2 stream in a nylon loop. Diffraction data were measured at –170 °C at beamline 5.0.2 at the Advanced Light Source (ALS) using a Quantum 4 CCD camera (Area Detector Systems Corp.) at a wavelength of 1.10 Å. Images were processed with DENZO[25], and the integrated intensities were scaled with SCALEPACK[25] using the default –3 σ cutoff.

Crystals of the THC–ERβ LBD complex were obtained by hanging drop vapor diffusion at 21–23 °C. Samples (2 μl) of a solution of the complex (4.8 mg ml^{-1}) were combined with 2 μl samples of a reservoir solution containing 1.5–1.75 M $(NH_4)_2SO_4$ and 100 mM sodium acetate, pH 4.8–5.2, and suspended over wells containing 800 μl of reservoir solution. The resulting crystals belong to the space group R3, with cell parameters a = b = 99.14 Å and c = 193.38 Å (hexagonal setting). The asymmetric unit contains two ERβ LBD monomers that do not form the dimer observed in the ERα complex. Instead, each of the two LBDs interacts similarly with symmetry-related molecules to form crystallographic trimers. Before data collection, a single crystal was transferred to a stabilizing solution (1.8 M $(NH_4)_2SO_4$, 100 mM NaCl, 100 mM sodium acetate, pH 4.5, and 10 μM THC). The crystal was then sequentially transferred at 30 min intervals through a series of solutions consisting of the stabilizing solution supplemented with increasing concentrations of ethylene glycol (1% (v/v) increments) to a final concentration of 15% (v/v). The crystal was then flash frozen in an N_2 stream in a nylon loop. Diffraction data were measured at –170 °C at beamline 5.0.2 at the ALS using a Quantum 4 CCD camera at a wavelength of 1.07 Å. Images were processed with DENZO, and the integrated intensities were scaled with SCALEPACK using the default –3 σ cutoff.

Structure determination and refinement. The model of the DES–ERα LBD–GRIP1 NR box II peptide complex (3ERD) was modified by truncating the side chains of the ligand-binding pocket of both monomers to Ala and by removing all ligands, waters, carboxymethyl groups and ions. After subjecting this edited model to rigid body refinement in REFMAC[26], the missing parts of the model were built. The rest of the model was corrected using MOLOC[27] and two-fold averaged maps generated with DM[26]. All masks for averaging were generated using MAMA[28], and PHASES[29] and the CCP4 suite[26] were used for the generation of structure factors and the calculation of weights. Initially, positional refinement was performed using REFMAC. At later stages, the model was refined using the simulated annealing, positional and B-factor refinement protocols in CNS[30]. All B-factors were refined isotropically. Anisotropic scaling and a bulk solvent correction were used throughout refinement. The R_{free} set contains a random sample of 6.5% of all data. All data between 47 and 1.95 Å (with no σ cutoff) were used. The current model is composed of residues 305–459 and 469–547 of monomer A, residues 305–460 and 472–547 of monomer B, residues 687–696 of peptide A, residues 686–695 of peptide B, two ligand molecules, 166 water molecules, one carboxymethyl group and one chloride ion. According to PROCHECK[26], 96.6% of all residues in the model are in the core regions of the Ramachandran plot, and none are in the disallowed regions.

The intensities within the ERβ data set fall off very rapidly as a function of resolution (Wilson B-factor ~90 $Å^2$ calculated from 4.5 to 2.95 Å). To increase the contribution of the higher resolution terms, the data were sharpened with a correction factor of -55 $Å^2$. Maps calculated using this sharpened data revealed higher resolution features, such as improved side chain density[31]. All subsequent manipulations were performed using this sharpened data.

The two LBDs in the asymmetric unit were located by molecular replacement in AmoRe[26] and TFFC[26]. The search model was constructed by overlapping the models of five ERα LBD complexes (PDB entries 1A52, 1ERE, 1ERR, 3ERD and 3ERT) and setting the occupancies of each model to 20% (R-factor = 55.3% and correlation coefficient = 55.9% after placement of both monomers). The model was then built using MOLOC and two-fold averaged maps generated with DM. MAMA was used for all mask manipulations, and PHASES and the CCP4 suite were used for the generation of structure factors and the calculation of weights. Refinement was performed initially using the positional refinement protocols in REFMAC and, later, using the simulated annealing, positional and B-factor refinement protocols in CNS. All B-factors were refined isotropically. Anisotropic scaling, a bulk solvent correction, and tight noncrystallographic symmetry restraints were used throughout refinement. The R_{free} set contains a random sample of 5% of all data. All data between 49 and 2.95 Å (with no σ cutoff) were used. The current model is composed of residues 261–284, 290–408 and 413–501 of monomer A, the last residue of the affinity tag and residues 256– 280, 294–410, 413–479 and 485–497 of monomer B, two ligand molecules, and nine water molecules. According to PROCHECK[26], 92.5% of all residues in the model are in the core regions of the Ramachandran plot, and none are in the disallowed regions.

Peptide binding assay. Samples of the GST–ERβ LBD fusion protein, in the absence or presence of the various ligands (at saturating concentrations), were mixed with an Leu-X-X-Leu-Leu motif-containing peptide (Ile-Leu-Arg-Lys-Leu-Leu-Gln-Glu), which had been N-terminally labeled with rhodamine (reaction buffer = 10 mM HEPES-Na, 150 mM NaCl, 2 mM $MgCl_2$, 1 mM EDTA and 100 μg ml^{-1} BSA, pH 7.9, and [peptide] = 5 nM). The binding reactions were incubated at ambient temperature with shaking for 1 h in 96-well plates (Whatman), and the fluorescence polarization was measured on an Analyst reader (Molecular Devices). K_d values were generated from triplicate assays by nonlinear least squares analysis (Prism, GraphPad Software).

Coordinates. Coordinates of the structures have been deposited in the Protein Data Bank (accession codes 1L2I and 1L2J for the ERα and ERβ complexes, respectively).

Acknowledgments

We thank T. Earnest for advice and assistance at beamline 5.0.2 (ALS is funded by the US Department of Energy Office of Basic Energy Sciences). We also thank M. Butte, N. Ota and Y. Shibata for assistance with data collection; P. Coward, A. Derman, and Y. Li for comments on the manuscript; and H. Deacon for extensive graphical assistance. This work was supported by the NIH (B.S.K, J.A.K. and D.A.A), the Howard Hughes Medical Institute (D.A.A.), the Susan G. Komen Breast Cancer Foundation (G.L.G.), the USAMRMC (G.L.G.) and the Illinois Department of Public Health (G.L.G). In the initial phases of this work, A.K.S. was supported by a Howard Hughes Medical Institute Predoctoral Fellowship and a UCSF Chancellor's Fellowship. All crystallographic studies were completed while A.K.S. was at UCSF, and the peptide binding studies were performed by A.K.S. at Tularik Inc.

Competing interests statement

The authors declare competing financial interests: see the Nature Structural Biology website (*http://structbio.nature.com*) for details.

Correspondence should be addressed to A.K.S. *email: ashiau@tularik.com* or G.L.G. *email: ggreene@uchicago.edu*

Received 1 August, 2001; accepted 8 February, 2002.

1. Katzenellenbogen, B.S. & Katzenellenbogen, J.A. *Breast Cancer Res.* **2**, 335–344 (2000).
2. Pettersson, K. & Gustafsson, J.A. *Annu. Rev. Physiol.* **63**, 165–192 (2001).
3. Meyers, M.J., Sun, J., Carlson, K.E., Katzenellenbogen, B.S. & Katzenellenbogen, J.A. *J. Med. Chem.* **42**, 2456–2468 (1999).
4. Sun, J. *et al. Endocrinology* **140**, 800–804 (1999).
5. Kraichely, D.M., Sun, J., Katzenellenbogen, J.A. & Katzenellenbogen, B.S. *Endocrinology* **141**, 3534–3545 (2000).
6. Pham, T.A., Hwung, Y.P., Santiso-Mere, D., McDonnell, D.P. & O'Malley, B.W. *Mol. Endocrinol.* **6**, 1043–1050 (1992).
7. Tzukerman, M.T. *et al. Mol. Endocrinol.* **8**, 21–30 (1994).
8. McInerney, E.M., Weis, K.E., Sun, J., Mosselman, S. & Katzenellenbogen, B.S. *Endocrinology* **139**, 4513–4522 (1998).
9. Barkhem, T. *et al. Mol. Pharmacol.* **54**, 105–112 (1998).
10. Danielian, P.S., White, R., Lees, J.A. & Parker, M.G. *EMBO J.* **11**, 1025–1033 (1992).
11. Berry, M., Metzger, D. & Chambon, P. *EMBO J.* **9**, 2811–2818 (1990).
12. Kraus, W.L., McInerney, E.M. & Katzenellenbogen, B.S. *Proc. Natl. Acad. Sci. USA* **92**, 12314–12318 (1995).
13. Steinmetz, A.C., Renaud, J.P. & Moras, D. *Annu. Rev. Biophys. Biomol. Struct.* **30**, 329–359 (2001).
14. Weatherman, R.V., Fletterick, R.J. & Scanlan, T.S. *Annu. Rev. Biochem.* **68**, 559–581 (1999).
15. Glass, C.K. & Rosenfeld, M.G. *Genes Dev.* **14**, 121–141 (2000).
16. Bourguet, W. *et al. Mol. Cell* **5**, 289–298 (2000).
17. Shiau, A.K. *et al. Cell* **95**, 927–937 (1998).
18. Brzozowski, A. *et al. Nature* **389**, 753–758 (1997).
19. Pike, A.C. *et al. EMBO J.* **18**, 4608–4618 (1999).
20. Pike, A.C. *et al. Structure* **9**, 145–153 (2001).
21. Shiau, A.K., Coward, P., Schwarz, M. & Lehmann, J.M. *Curr. Opin. Drug Discov. Devel.* **4**, 575–590 (2001).
22. Singh, S.M., Gauthier, S. & Labrie, F. *Curr. Med. Chem.* **7**, 211–247 (2000).
23. Souque, A. *et al. Endocrinology* **136**, 5651–5658 (1995).
24. Mangelsdorf, D.J. *et al. Cell* **83**, 835–839 (1995).
25. Otwinowski, Z. & Minor, W. *Methods Enzymol.* **276**, 307–326 (1997).
26. Dodson, E.J., Winn, M. & Ralph, A. *Methods Enzymol.* **277**, 620–634 (1997).
27. Muller, K. *et al. Bull. Soc. Chim. Belge.* **97**, 655–667 (1988).
28. Kleywegt, G.J. & Jones, T.A. *Acta Crystallogr. D* **55**, 941–944. (1999).
29. Furey, W. & Swaminathan, S. *Methods Enzymol.* **277**, 590–619 (1997).
30. Brünger, A.T. *et al. Acta Crystallogr. D* **54**, 905–921 (1998).
31. Stehle, T., Gamblin, S.J., Yan, Y. & Harrison, S.C. *Structure* **4** 165–182 (1996).
32. Esnouf, R.M. *J. Mol. Graph. Model.* **15**, 132–134, 112–113 (1997).
33. Merritt, E.A. & Bacon, D.J. *Methods Enzymol.* **277**, 505–524 (1997).
34. Kleywegt, G.J. & Jones, T.A. *Methods Enzymol.* **277**, 525–545 (1997).